UNIVERSITY OF CALIFORNIA,
IRVINE

System Design Strategy & Energy Yield Analysis

for Solar PV Application in an Urban Community with Constrained Rooftop Area

THESIS

submitted in partial satisfaction of the requirements
for the degree of

MASTER OF SCIENCE

in Mechanical and Aerospace Engineering

by

Yanchen Wu

Thesis Committee:
Professor Jack Brouwer, Chair
Professor Yun Wang
Assistant Professor Jaeho Lee

2020

Dedication

To

my parents and friends

in recognition of their worth and support

a deep apperaction

Success depends upon cautious preparation and critical analysis,
and without such assertive actions
there is sure to be failure; a decisive man acts
before he speaks,
and afterwards speaks according to his action.

Analects of Confucius
Confucius

and be ready

It is not difficult to know a thing;
what is difficult is to know how to use what you know.

Han Feizi
Han Fei

Table of Content

Page

List of Figures

Page

List of Tables

Page

Nomenclature

a_M Module inclination angle with respect to the horizon

A_M Module azimuth angle with respect to the north

a_S Sun altitude angle

A_S Sun azimuth angle with respect to the north

a_r The roof pitch angle

a_{m_f} The tilting angle of the front row module respect to the roof surface

a_{m_b} The tilting angle of the back row module respect to the roof surface

D The distance between the bottom edge of the front row module and the bottom edge of the back row module

E_b POA beam irradiance

E_d POA sky-diffuse irradiance

E_g POA ground-reflected irradiance

E_{POA} Total plane of array irradiance

GVF Ground View Factor

I_{DNI} Direct normal irradiance

I_{DHI} Diffuse horizontal irradiance

I_{GHI} Global horizontal irradiance

SVF Sky View Factor

S_1 The distance from the bottom module edge to the roof projection of the upper module edge on the roof surface of the front row module

S_2 The length of the vertical shadow projection of the upper module edge of the front row module onto the rooftop surface

S The summation of S_1 and the maximum value of S_2

SA The shaded area on the module

SF The shading factor of a module

R The point of intersection of sunray and back row module surface

T The point of the top edge of the front row module

P_0 The point of intersection of the horizontal line extended from the top module edge of the front row to the surface of the back row module

P Any point on the back row surface between the bottom edge and P_0 of the back row module

L The length of the side of the module that is along the direction of the longest roof edge

W The length of the side of the module that is perpendicular to the direction of the longest roof edge

U The distance from the bottom edge of the back row module to the intersection line of the planes of sunray and roof surface

x The length of self-shading from the bottom edge to the endpoint of shading on the module surface of the back row module

y The distance from the bottom edge of the back row module to any point P, that is below the point P_0

α Angle of incidence

α_r The angle between sunray and roof normal

α_m The angle between sunray and module normal

θ Angle between the plane of sun sunray and the plane of the oof surface

ρ Albedo factor

ϕ Portion of the sky that is exposed to the module at any point along y

σ The angle between the vector $\overrightarrow{PT}$ and the unit vector in the negative x-direction

$\overrightarrow{Vs}$ The unit vector of sunray

$\overrightarrow{Nr}$ The unit vector of the roof normal

$\overrightarrow{Nm}$ The unit vector of the module normal

Acknowledgments

I would like to express the deepest appreciation to my committee chair, Professor Jack Brouwer, who has the attitude and knowledge of a genius: he continually and convincingly conveyed a spirit of adventure in regard to research and scholarship, and an excitement in regard to teaching. Without his guidance and mentorship, this thesis would not have been possible.

I would also like to thank my committee members, Professor Yun Wang and Professor Jaeho Lee, who offered help to review my thesis, with their valuable time and effort.

I would also like to thank Dr. Robert J. Flores for his excellent leadership in research and constructive criticism on the academic work that I have been producing during my career as a researcher.

In addition, a thank you to Professor Scott Samuelsen along with Professor Jack Brouwer for providing me with the valuable opportunity to join the Advanced Power and Energy Program.

In the end, I would like to thank my colleagues with whom I have had the honor of working on various projects. I am humbled by your talent and dedication.

Abstract of the Thesis

System Design Strategy & Energy Yield Analysis

for Solar PV Application in an Urban Community with Constrained Rooftop Area

By

Yanchen Wu

Master of Science in Mechanical and Aerospace Engineering

University of California, Irvine, 2020

Professor Jack Brouwer, Chair

As the State of California sets up ambitious goals to encourage the use of renewable energy, urban communities in California are starting to adopt community-wide solar photovoltaic (PV) projects with onsite generation. However, with the limited installation space and various structural conditions of rooftops in the community, the total available area to install a solar PV system is severely constrained. The aim to effectively offset the peak of the electricity usage of the community and the goal to increase renewable energy penetration could both be significantly limited. In this work, much in-depth analysis of solar PV installation and layout plans to maximize energy yield and to boost economic return is performed. Besides constant tilted PV array configuration, a novel PV installation layout, the incremental tilted layout, is proposed. For the constant tilted array, with maximum rows of module placed on the rooftop, it is desired to tilting the array at a low angle for roof pitch below local optimal tilt. Also, the low incremental tilting angle can achieve similar energy yield as the constant tilted array but could bring better economics return on a rooftop with low pitches. Meanwhile, a series of constructive strategies to effectively

design a community solar PV project is proposed. The Oak View community at Huntington Beach is used as an example to demonstrate the proposed strategy. A community zone-map to deploy PV is created based on the location of critical electrical infrastructures. Overall, it is found that the weather condition and load profile can each significantly affect the solar penetration of the community.

1. Introduction

The state of California has set up aims to increase zero-carbon electricity generation. The bill SB-100 has set a mandate for the state to reach 65% renewable electricity by 2030 and 100% by 2045 [1]. Community solar pilot projects such as the Advanced Energy Community [2] [3] could become a potential direction for PV project development in the states of California. For typical solar PV projects, the goal is to maximize the solar system output per panel, minimizing the cost of electricity. The yield of a PV module is affected by several factors, predominantly the environment, the location, and the layout configuration [4] [5]. Module orientation, row spacing, and panel inclination angle are crucial factors in analyzing the amount of solar energy that can be converted to electricity for a solar module [4] [6].

The optimal angle of PV tilting at various azimuth has been well researched and identified in the past for the constant tilted PV array at various geological location around the world [7] [8] [9]. The optimal angle only serves as a general reference and it is a value for an individual module to locally achieve maximum annual irradiation [10]. At the optimal azimuth and tilting angle, it reaches the balance between direct and sky-diffuse irradiation to maximize total irradiance received by the plane of the solar PV array. Some papers recommended the array to tilt close to the value of the latitude angle as a simplified way to obtain the optimal tilting angle.

The shading and blocking effect are the two most important factors that will affect the quantity of irradiance strikes on the modules and how the I-V curve of the module could be affected [4] [5]. More attention is needed in a multi-row PV array to balance off the total module quantity that can be fitted on a target surface and the row space [4]. The row distance within the PV array is crucial and the value is typically determined from avoiding the occurrence of any shading during the

effective solar hours around the year. Thus, the distance between rows is set to be the minimum distance to avoid self-shading on the winter solstice day from 10 AM to 3 PM [4].

The Maximum Power Point Tracker is an essential component to always ensure the inverter to harvest the maximum amount of DC energy from modules, right before DC power is converted to AC inside the inverter. During the maximum power tracking process, the module-level inverter usually outperforms the string-level inverter if non-uniform shading occurs [11] [12].

The general design and modeling methodology are goal-oriented that are either to maximize the total energy yield from an array for a designated area regardless of the cost and payback period or to maximize the panel economics of the entire array thus accelerate the project cash flow or investment payback period. In certain scenarios, such as designing a solar PV system in an urban area with a relatively high energy use intensity and limited rooftop area could be challenging [13] [14] [6]. Thus a comprehensive study to discover the balance total between energy yield and system economics especially on area-constrained surfaces in the urban location could be beneficial for the community project development [15].

Much of the prior work has been focusing on maximizing the energy yield of either flush mounted or the constantly tilted PV array with the major aim to reduce the electric bill of target building [16]. This prior work, however, has not examined maximizing solar output when designing a system for a fixed or constrained area, i.e., a roof surface or fixed area plot of land. In addition, the prior work has not been able to effectively come up with a new method of PV array layout on tilted surfaces. In certain scenarios of an urban area or city district, it is more often desired to design a renewable energy system that could achieve ZNE (Zero Net Energy) while finding the balance between maximizing the total energy harvest and the array economics with space limited rooftop surfaces.

The current work explores this question of solar array design for a constrained area by introducing a new PV array layout method, the incremental tilted layout, and developing a PV energy simulation model with Maximum Power Point Tracking (MPPT) included. This model is used to simulate and optimize the amount of DC energy production under pre-decided configurations such as but not limited to azimuth, tilt, row spacing, roof pitch, and area, as well as the incremental tilting angle if the array is designated to be an incrementally tilted array. The calculation has the resolution on an hourly basis for an entire calendar year and includes the sub-module-level shading effect on the module electrical performance of the PV array. The model allows the simulation to specify the cardinal directions and pitches of a dimension specified rooftop. The analysis presented in the work is performed based on various pitched rooftops ranging from 0° to 30° with a south-facing surface at the location of southern California (33.67°N, 117.87°W) [17].

The newly proposed PV array layout in this work are compared with the classical layout solution. Meanwhile, the array energy yield and the array economics are both calculated and presented to provide the basic relationship between array and roof parameters. A comparative analysis is made among various array layout approaches.

Nowadays, many commercial solar PV design software are available to simulate PV energy yields, such as the famous PVSyst and PVWatts software. However, many solar project development industry usually requires fast and accurate design response to the customers for a residential solar system without or with the limited number of field trips to the installation site. In addition, the traditional solar simulation software such as PVSyst and PVWatts could not easily visualize the dimension, orientation, or rooftop obstructions thus creates inconvenience for rooftop PV designers. Therefore, the new generation of solar design software such as Helioscope [18] combines the energy simulation and satellite image together to create an enhanced and visualized

design environment for the designers without going to the site to analyze the rooftop conditions. For a large community with hundreds of building rooftops, site commissioning from one building to another could take a significant amount of time, thus the utilization of such a tool could be much easier to assess the PV installation potential and generate accurate energy yield based on the resolution of input weather data. The modeling procedure of utilizing such software is important for PV design in a large community and will be analyzed in detail in this work.

Meanwhile, with the appropriate design tool in hand, merely applying the method of designing a single solar PV system in a large multi-functional community would still be a challenging task. Therefore, specific design procedures are required to systematically assess the community's PV installation and energy production potential. For a community PV project, the constant modification of the design is highly possible. Thus, the organization and categorization of the design are crucial for a community project based on specific consideration such as the location and limitation of electrical infrastructures. Many design scenarios regarding a community project are required in order to comprehensively analyze the PV deployment potential with various design considerations. A sample community is introduced in this work with detailed design procedures applied to better understand the general methodology proposed to design a community-wide solar PV project.

In order to increase renewable energy utilization in the community, solar production and community electricity demand both need to be analyzed. Once the solar production profile is affected by various weather conditions, the net-demand will change, which represents the intermittency of renewable energy. For a multi-functional community including commercial, industrial, school, and residential, the energy load schedule could vary significantly. The shape of the daily load profile for residential and industrial could be totally different. Therefore, in order to

increase renewable energy penetration and reduce the curtailment, it is important to analyze the shape and magnitude of the load and solar production profile to better propose the specific community PV design solutions such as array orientation and the location of deployment. In addition, the solar production profiles from various seasons, month, day, and even hour requires detailed analysis to successfully understand the variability of the overall net-demand of the community. Overall, this work could provide insights and suggestions on designing and constructing a zero-net-energy community powered by solar PV.

2. Solar PV Energy Modeling & Simulation

The solar irradiance is introduced in this section, and the irradiance received by the array the solar PV array is the Plane of Array (POA) irradiance [19] [20], which consist of three components and are presented with detailed equations. The coordinate system of calculating solar irradiance is also introduced here as well.

2.1 Model of Solar Irradiance

In order to carry out the simulation, principles of celestial mechanics were applied. The Celestial semi-sphere was used to parameterize the position and motion of every celestial object with the azimuth and altitude angle. For this work, the PV module is at the center of the sphere (indicated as the observer in Figure 1), and the fundamental plane is at the horizon of the panel (the horizontal coordinate system). The outcome is a coordinate system used to express the sun position with two angles: azimuth angle and altitude angle (see Figure 1). The Azimuth angle starts from 0° in the north and follows the clockwise direction passing through 90° east, 180° south, 270° west, and back to the north. The altitude angle starts from the ground ranging from 0° to 90°.

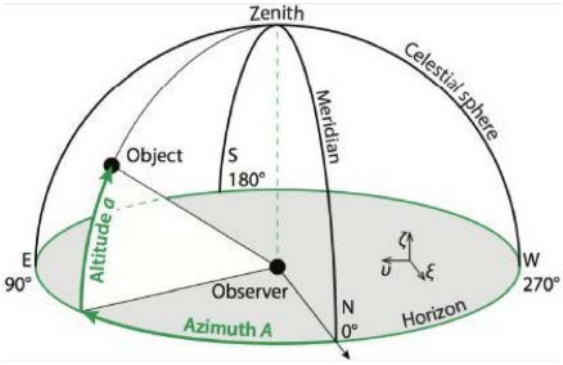

Figure 1. Celestial semi-sphere and horizontal coordinate system [21]

The solar irradiance is composed of two components, the direct normal irradiance (I_{DNI}) and the diffuse horizontal irradiance (I_{DHI}). Smets et al [21] demonstrate how to calculate the amount of irradiance on a PV module. However, the amount of irradiance on a PV module or array is

governed by the Plane of Array (POA) irradiance. The total POA irradiance (E_{POA}) contains three components: the POA beam irradiance (E_b), POA sky-diffuse irradiance (E_d), and POA ground-reflected irradiance (E_g). POA irradiance and the components is shown in Equation (1) [19]

$$E_{POA} = E_b + E_d + E_g \quad (1)$$

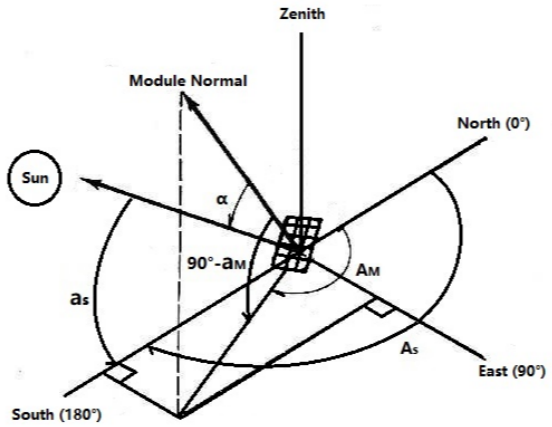

Figure 2. Sun position and module orientation with the angle of incident [22]

2.1.1 POA Beam Irradiance

The amount of POA beam irradiance that strikes on a solar panel is determined by direct normal irradiance (DNI) and the angle of incidence, which is the angle between the sun position and the normal vector of the module surface. The module position can be expressed by the direction of the module normal in horizontal coordinates system (A_M, a_M), in which A_M is the azimuthal angle from the north and a_M is the inclination angle regarding the horizontal direction, shown in Figure 2. Sun position can be parameterized in a similar fashion (A_s, a_s), by the azimuth angle A_s and the altitude angle a_s. Therefore, the POA beam irradiance on a module is given by the Equation (2) [19].

$$E_b = I_{DNI} \cdot \cos(\alpha) \quad (2)$$

Where I_{DNI} represents the direct normal irradiance and α is the angle of incidence (AOI) between the normal of the module and the sun position show, which can be calculated by Equation (3) [19]:

$$\cos(\alpha) = \cos(a_M)\cos(a_S)\cos(A_M - A_S) + \sin(a_M) \cdot \sin(a_S) \quad (3)$$

2.1.2 POA Sky-Diffuse Irradiance

Diffuse radiation accounts for the radiation of the sun that has been scattered by molecules, particles, and aerosols in the atmosphere. It is also proportional to the *sky view factor* (*SVF*) [21]. The component E_d in Equation (4) [19] is a function of diffuse horizontal irradiance (I_{DHI}) and the angle (φ) of the portion of the sky that is exposed to the module surface.

$$E_d = I_{DHI} \cdot SVF \quad (4)$$

In order to compute the amount of diffuse radiation striking the panel, isotropic (uniform) sky diffuse condition is applied. This condition assumes that the entire sky dome emits the diffuse radiation uniformly, neglecting horizon diffuse brightening and circumsolar diffuse radiation. A comparative study was done between the isotropic and anisotropic models for solar radiation estimations on a sloped surface, and the results showed that the isotropic model (also known as the LJ-method) gives better estimates and reduces statistical errors [23]. The sky view factor (*SVF*) is calculated in (5) [19]. The formula for the diffuse radiation of a tilted surface is given in Equation (6) [19]

$$\text{SVF} = \left[\frac{1 + \cos(180° - \varphi)}{2}\right] \quad (5)$$

Thus, the sky-diffuse irradiance can be calculated from (6),

$$E_d = I_{DHI} \cdot \left[\frac{1 + \cos(a_M)}{2}\right] \quad (6)$$

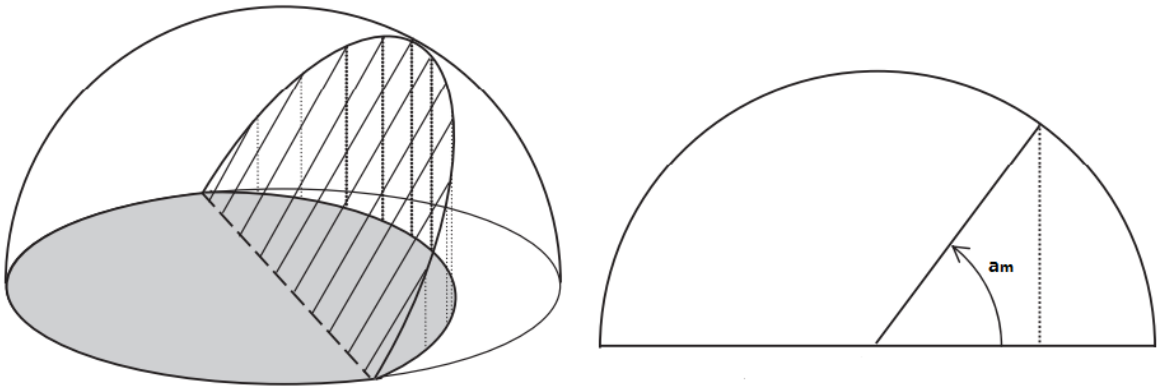

Figure 3. The sky-view factor approximation as the area of the projection of part of the hemisphere to the horizontal surface [24]

For a slope of the inclination angle of a_M, the portion of the sky available will be the projection of it with a gray portion shown in Figure 3. Note in the Equation (6), if there is a horizontal surface ($a_M = 0°$) all portion the sky will be available to it, with an SVF value of 1. If $a_M = 90°$, then only half of the sky will be in front, thus the POA Sky-Diffuse irradiance will also be halved [25].

2.1.3 POA Ground Reflected Irradiance

The reflected radiation is the solar radiation that has reflected off the ground or on a surface in front of the collector. This type of radiance is based on the albedo coefficient (a ratio of reflected irradiance regarding incident radiance) and its formula is given by Equation (7) [21] [20].

$$E_g = I_{GHI} \cdot \rho \cdot \left[\frac{1 - \cos(a_M)}{2}\right] \tag{7}$$

Where ρ represents the albedo factor, which is a constant value that depends upon the type of surfaces and environment around the sloped surface [23]. Different locations and surfaces will have different albedo values. For example, 0.2 is used for a hot and humid tropical location, 0.5 for dry locations and 0.9 for ground covered with snow [26]. Since the analysis in this work focused on the urban environment, resulting in a small albedo factor (i.e. 0.1), thus E_g is very small when compared to diffuse and beam irradiance [27]. Also, the albedo factor largely varies for different seasons, locations, and the surrounding environment.

2.2 Self-Shading Simulation

The solar irradiance received by an array heavily depends on the types of the racking and layout. In this work, for the incremental tilted array, changing the row distance could significantly affect both E_b and E_d due to self-shading and self-blocking effect. These effects will be considered and modeled when determining the total plane of array irradiance (E_{POA}). For the incremental tilted array, since the tilting angle for each row is different, the longest non-shaded row space for each row is calculated from 10 AM to 3 PM on December 21st, the winter solstice [28].

In order to effectively model the shading effect on the solar module, it is necessary to convert the horizontal coordinate system to the Cartesian coordinate system. North (0°) and east (90°) indicate the positive direction of the i and j unit vectors, and the cross product of i and j (or the vector perpendicular to the surface of the earth), indicates unit vector k. In this Cartesian coordinate, three vectors are important to express: sunray, roof normal, and panel normal. The unit vector with components < i, j, k > of a sunray can be expressed as:

$$\overrightarrow{Vs} = <\ \cos a_s \cdot \sin A_s\,, \cos a_s \cdot \cos A_s\,,\ \sin a_s > \tag{8}$$

The unit vector of the roof (or module) normal can be expressed as:

$$\overrightarrow{Nr} = <\ \sin a_r \cdot \sin A_r\,, \sin a_r \cdot \cos A_r\ ,\ \cos a_r > \tag{9}$$

The angle α_r (or α_m) between sunray and roof normal (or module normal) can be found by applying dot product of the vectors of sunray $\overrightarrow{Vs}$ and the roof normal $\overrightarrow{Nr}$ (or $\overrightarrow{Nm}$) for each hour of the day while a_s is greater than zero.

Assuming panel thickness is neglected and only one panel exists in each row to best study the shading phenomena. The longest non-shaded distance S between two adjacent rows on December 21th as shown in Figure 4 is calculated as follows:

$$S_1 = L \cdot \cos a_{m\_f} \tag{10}$$

The length of the projection of sunray unto roof plane at a different time can be expressed as:

$$Proj_{sunray}^{t}(roof) = L \cdot \sin a_{m\_f} \cdot \tan \alpha_r^t \qquad if(\,|A_s^t - A_r| < 90°) \tag{11}$$

The vertical and horizontal component of the projection on the roof plane is:

$$Proj_{s\_r\_v}^{t} = Proj_{sunray}^{t}(roof) \cdot \cos|A_s^t - A_r| \tag{12}$$

$$Proj_{s\_r\_h}^{t} = Proj_{sunray}^{t}(roof) \cdot \sin|A_s^t - A_r| \tag{13}$$

Thus, S_2^t can be determined as:

$$S_2^t = \begin{cases} W \cdot \tan\left(90° - \left|A_s^t - A_f\right|\right), & Proj_{s\_r\_h}^{t} > W \\ Proj_{s\_r\_v}^{t}, & Proj_{s\_r\_h}^{t} \le W \\ 0, & |A_s^t - A_r| \ge 90° \end{cases} \tag{14}$$

So, S can be expressed as the sum of S_1 and the maximum value of S_2^t from 10 AM to 3 PM on Dec 21th:

$$S = S_1 + \max\,(S_2^t) \tag{15}$$

As the distance between modules decreases from the non-shaded position, a portion of the module will be shaded at different times of a year. As shown in Figure 4, the length of vertical shading (x) is defined to be from the bottom edge to the top edge, and the quantity that measures the shading of the back row can be expressed by a shading factor (SF), which is the ratio of the shaded area of module over module area.

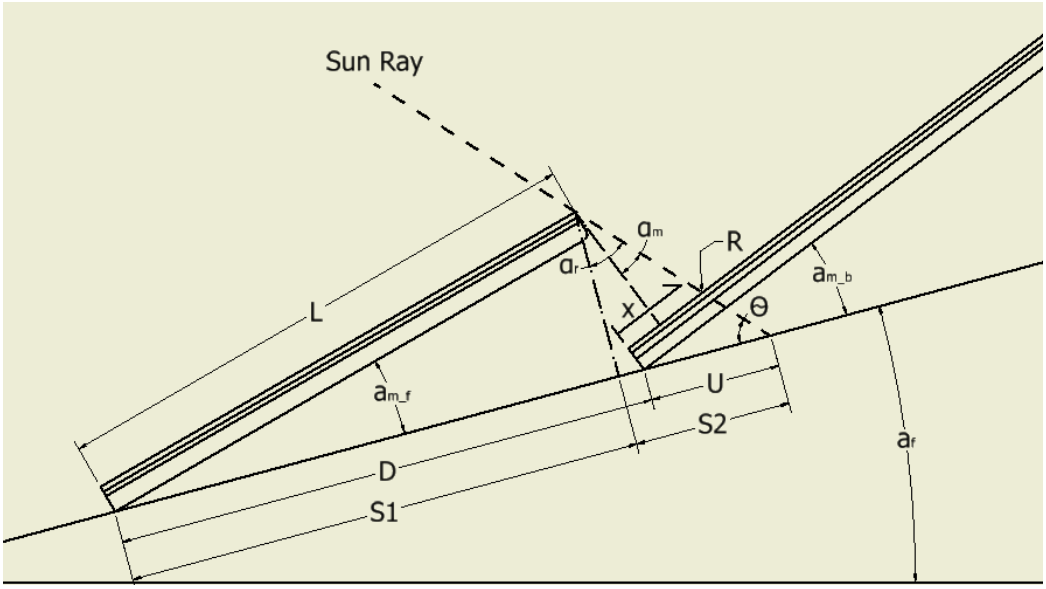

Figure 4. Parameters required to establish the shading model of each module in a PV array

The shaded area of the front module onto the back module at any given time can be determined by finding x and the shape of the shade of either a triangle or trapezoid and assume the azimuth of the module is the same as the roof azimuth. Thus x can be defined by determining the module tilt angle of the back module a_{m_b} (assume the front module is tilting at a_{m_f}), the angle θ between the planes of sunray and roof for any time, and the distance U from the bottom edge of the back module to the intersection point of the planes of sunray and roof as shown in Equation (18):

$$U = \begin{cases} S - D, & S > D \\ 0, & S < D \end{cases} \tag{16}$$

$$SF^t = 0, \qquad if\ (U = 0) \tag{17}$$

$$x^t = \frac{U \cdot \sin\theta^t}{\sin(180° - \theta^t - a_{m\_b})}\ , \quad if\ (|A_s^t - A_r| < 90°) \tag{18}$$

Thus, the shaded area (SA) onto the back row module can be categorized as either a trapezoid or a triangle shape based on the length of the horizontal projection of sunray onto the plane of the back row module ($P_{s\_m\_h}^t$):

$$SA^t = \begin{cases} \left(W - P^t_{s\_m\_h}\right) \cdot x^t + \dfrac{(x^t)^2}{2 \cdot \tan(90° - |A^t_s - A_r|)}, & W > P^t_{s\_m\_h} \\ \dfrac{(x^t)^2}{2 \cdot \tan(90° - |A^t_s - A_r|)}, & W \le P^t_{s\_m\_h} \end{cases} \quad (19)$$

Thus, the shading factor (shaded area over model surface areas) of a module SF can be calculated easily:

$$SF^t = \frac{SA^t}{W \cdot L}, \quad if\ (U \neq 0) \quad (20)$$

The angle between module normal and sunray is calculated as α_m, which is mentioned earlier in this section. If the absolute value between the roof and sunray azimuth angle is equal to or larger than 90°, the shading facto can be expressed as:

$$SF^t = \begin{cases} 1, & \left|A^t_s - A_f\right| \geq 90° \ and\ \alpha_m \geq 90° \\ 0, & \left|A^t_s - A_f\right| \geq 90° \ and\ \alpha_m < 90° \end{cases} \quad (21)$$

2.3 View Factor

The view factor of any point on a solar module indicates the available portion of the total irradiance from the sky or from the ground. The view factor is a very important concept of consideration of solar PV array layout, especially when the row to row distance of the solar PV array is significantly small, and thus the total diffuse irradiance received by the array highly depends on the view factors.

2.3.1 Sky View Factor

As Figure 5 shows, for the incremental tilted array, the tilting angle of each row increases by a constant, thus the average SVF also changes from row to row. Meanwhile, the portion of the sky that is exposed to the back row module could be affected largely by the tilting angles of the front and back rows.

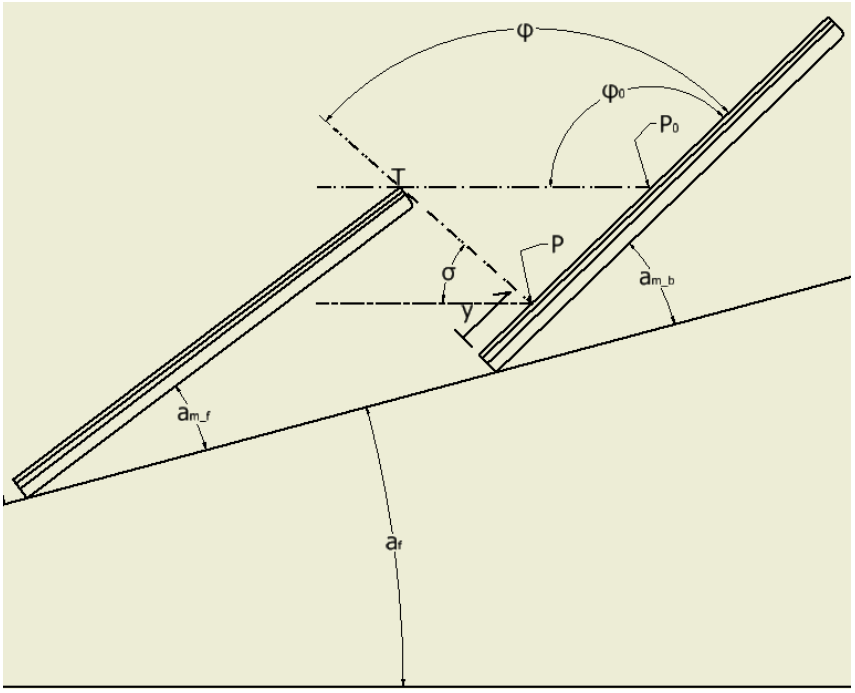

Figure 5. Parameters required to establish and calculate the sky view factor of each module in a PV array

Assuming that any point P on the surface of the back row module that is between the bottom edge and P_0, is expressed as the distance y, and the length from the bottom edge to the point of P_0 can be expressed in Equation (22). The angle φ at the point P on the surface of the module as shown in Figure 5 is defined by the module tilt respect to the ground and the top edge point T of the front module. Thus, the average SVF of the back module can be determined by constructing a two-dimensional x-y coordinate system with the origin at the bottom edge of the back row module to determine the angle σ and φ.

$$P_0 = \frac{L \cdot \sin(a_{m\_f} + a_r) - D \cdot \sin a_r}{\sin(a_{m\_b} + a_r)} \tag{22}$$

Point T and point P in the coordinate system can be expressed as:

$$P = \left(y \cdot \cos(a_{m\_b} + a_r)\ , y \cdot \sin(a_{m\_b} + a_r)\right) \tag{23}$$

$$T = (L \cdot \cos(a_{m\_f} + a_r) - D \cdot \cos a_r\ , L \cdot \sin(a_{m\_f} + a_r) - D \cdot \sin(a_r)) \tag{24}$$

The angle σ between vector $\overrightarrow{PT}$ and the unit vector in the negative x-direction can be determined with dot product operation. Thus, the average SVF of the back module can be calculated as:

$$\varphi = 180° - (a_{m\_b} + a_r + \sigma) \tag{25}$$

$$\overline{SVF} = \frac{1}{L} \cdot \left[\int_0^{P_0} \left[\frac{1 + \cos(180° - \varphi)}{2} \right] dy + (L - P_0) \cdot \left(\frac{1 + \cos(a_{m\_b} + a_r)}{2} \right) \right] \tag{26}$$

2.3.2 Ground View Factor

The ground view factor (GVF) is calculated based on the portion of the ground that is available and can reflect irradiance from the ground to the module. The original assumption made about the GVF is that the horizon blocking and near field shading is ignored. However, in this work, the solar modules are closely placed, and this portion of the module that is still available from the reflected irradiance from the ground can be determined with a simplification of area fraction for rows other than the first row.

$$\overline{GVF} = \left(\frac{W \cdot (L - P_0)}{W \cdot L} \right) \cdot \left[\frac{1 - \cos(a_M)}{2} \right] \tag{27}$$

2.4 Total Irradiance on PV Array

The total irradiance of the array is the summation of the total POA irradiance striking on every individual module in the array on that roof surface.

The total POA irradiance received by the array with N rows for the entire calendar year (8760 hours) is calculated as:

$$E_{Array\_Total\_POA} = \sum_{t=1}^{8760} \sum_{n=1}^{N} E_n^t \tag{28}$$

Where, E_n is indicated as the total irradiance received by the nst row module:

$$E_n^t = W \cdot L \cdot [E_b^t \cdot (1 - SF_n^t) + I_{DHI}^t \cdot \overline{SVF_n} + I_{GHI}^t \cdot \rho \cdot \overline{GVF_n}] \tag{29}$$

2.5 Weather and Module Data

The input of the model is based on the hourly metrological data obtained from NREL as Typical Meteorological Years Version 3 (TMY3) files, which contain irradiance data such as GHI, DHI, and DNI. The data used is collected by John Wayne Airport located in southern California from 1991-2005 [29] [30] [31]. The chosen solar module is GCL-M6/72 355W, and the data such as length, width, short circuit current, open-circuit voltage, cell number, temperature coefficients, and so on are taken from the datasheet of the manufacturer shown in the table below [32].

Table 1. Parameters obtained from the selected PV panel manufacturer datasheet

Panel Parameter	Value
Open Circuit Voltage	47.20 V
Short Circuit Voltage	9.73 A
Temperature Coefficient of Isc	+0.06%/°C
Temperature Coefficient of Voc	-0.30%/°C
Number of Cells	72
Length	1.956 m
Width	0.992 m

2.6 Local optimal Inclination & Azimuth Orientation

The results on different PV system layouts and how PV module layout parameters affect the irradiance received on the panels are presented in this section. The tilt angle for that maximizes POA irradiance versus azimuthal angle for a latitude of 33.7˚ N is shown in Figure 6 (0^o azimuthal angle corresponds to north-facing). For example, a north-facing panel receives maximum irradiance when mounted flat on the ground, or 0^o tilt. Likewise, the single south-facing panel receives maximum irradiance when tiled at 24.3°. Figure 6 also splits between direct and diffuse radiation. Note that these results are only applicable for a single module, not a set of modules installed in rows. In this instance, the optimal angle can change due to changing SVF.

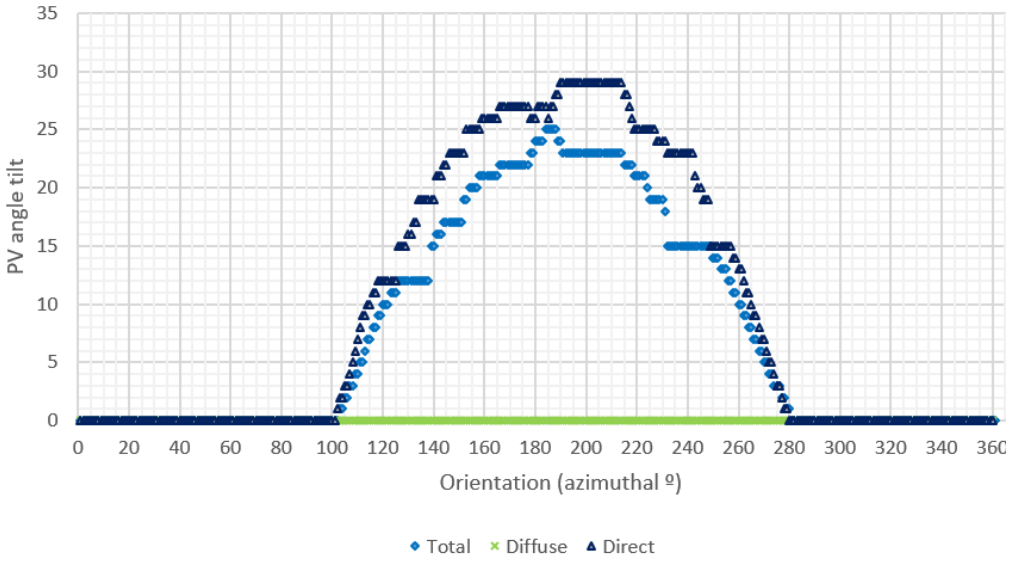

Figure 6. Optimum tilt angle for panel with orientations at latitude of 33.7˚

According to the model results, the diffuse radiation is always maximized when laying the panel flat, whereas direct radiation is maximized at an angle equal to or a little bit higher than the actual optimal angle (for an azimuthal angle of 180º, direct irradiance is maximized with a tilt between 27º and 30º). Based on these results, when panel orientation is approximately between 0-100° and 280-360°, panels should be mounted with no tilt. On the other hand, for roof facing south (180°, a typical azimuthal orientation for many buildings) and southwest, an inclination of 23-25° is desired at latitude 33.7°N.

2.7 PV Module & MPPT Electrical Modeling

The electrical portion of this work includes both string leveled and module leveled MPPT devices. The effect of sub-module partial shading on the I-V curve is modeled, assuming each module used contains three bypass diodes. The MPPT tracks the maximum DC power point of each module and then the total max DC power for the array on the roof is summed. The details of establishing the partial shaded I-V and P-V curve for solar modules have been extensively modeled with methods and equations [33]. The annual maximum energy for the array is that of the summation of each

row of the module in the array on an hourly basis. It has been analyzed by many research that under partial shading conditions, the module placed in landscape orientation produces higher energy than portrait orientation [34]. Therefore, each row of the module will be placed in a landscape fashion. It is important to note in this work, the DC power output is based on an hourly basis. As mentioned earlier in the shading section in order to simplify the calculation on shading and electrical, each row only contains one module and all the rows are connected in parallel when the string inverter is used.

2.7.1 Submodule-Level I-V & P-V Curve Simulation

Since the weather data used is collected from John Wayne Airport in Southern California, the annual optimal tilt for a single unshaded module at 180° facing is approximately 27-29° [17]. Since panel performance and economics depend on orientation, surface slope affects panel installation. For this section, a rectangular south-facing (180°) rooftop segment, with the constrained area (10.9 m long and 2 meters wide), and a pitch ranging from 0° to 30° in 5° increments is analyzed. The types of module layout include both constant and incremental tilt, or where subsequent panel rows are tilted at a higher pitch than preceding panels. Note that the tilt options include a flush mount where the modules are parallel to the mounting surface.

In order to avoid shading, most solar developers have considered using the longest shading distance that occurs on the winter solstice from 10 AM to 3 PM local time to set the row to row distance for the non-shaded PV array during effect solar hours throughout a year [28]. Thus the minimum row to row distance presented in this work follows this standard industrial practice.

For the solar module GCL-M6/72-355W used, the unshaded module under 1000 W/m^2 and at 25°C with 3 bypass diodes, has a modeled I-V and V-P curve shown in Figure 7.

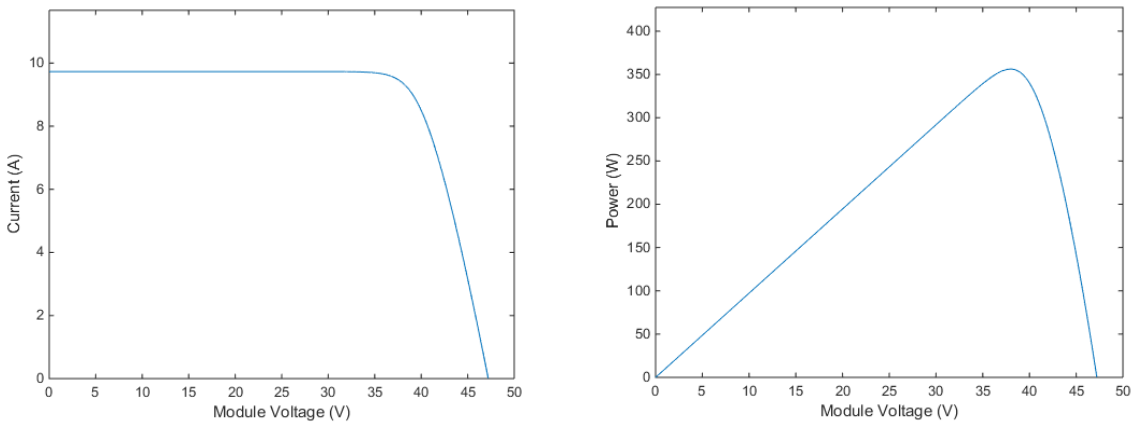

Figure 7. The I-V and P-V curve of GCL-M6/72 355W module under 25°C and 1000W/m²

If three sub-modules, each with a bypass diode, are under three different shading conditions such as 800W/m², 500W/m², and 200W/m² at 35C°, the generated Figure 8 demonstrates modeled results of the I-V and V-P curve under such conditions. The partial shading is modeled based on equations and methods in an article [35].

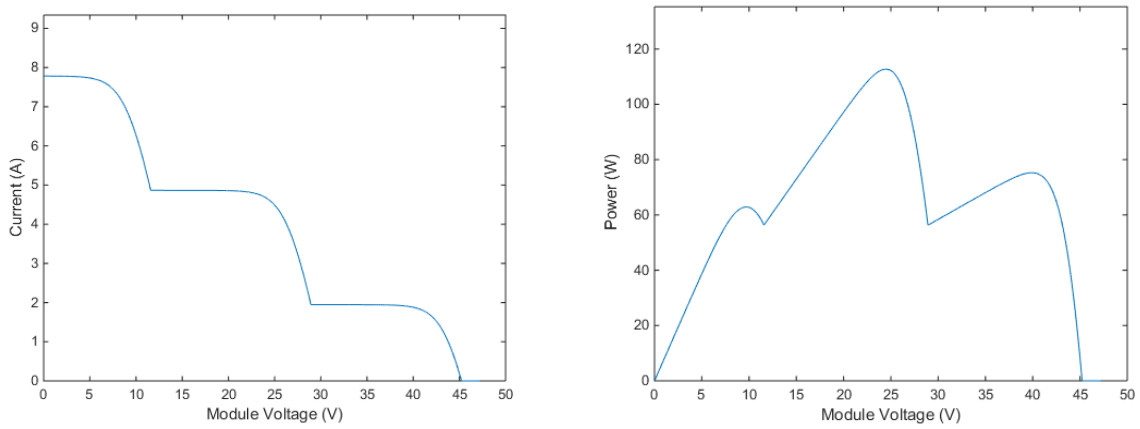

Figure 8. The I-V and P-V curve of GCL-M6/72 355W module with three sub-module under 800W/m², 500W/m², and 200W/m² respectively at 35C°

The DC MPPT device is assumed to be always capable of tracking the maximum DC power of each module at every single hour under different shading and temperature condition [36] throughout the year. Since the aim is to maximize DC energy produced from an area-constrained

array, the row to row distance will be set based on the percentage row distance reduction (PRDR) from the non-shaded distance (i.e. 30% PRDR indicates 30% of the row distance reduction from the original non-shaded distance, which is 0%).

3. Constant Tilted solar PV Array on an Area-Constrained Surface

In this section, the analysis of the fixed tilted solar array with a uniform tilting angle is introduced, all of the modules with the same tilt with respect to the rooftop surface. The constant tilted PV array is one of the most common tilting options for rooftop PV installation. The shading and irradiance of the PV array are calculated and analyzed.

3.1 Irradiance Analysis of a South Facing 15° Pitched Rooftop

The irradiance on the constant tilted solar PV array on the rooftop with 15° pitch is presented in this sub-section. Various tilting angle with respect to the surface is applied to better analyze the irradiance level. The distance of rows are also indicated as a varioable to simulate the shading condition on the array.

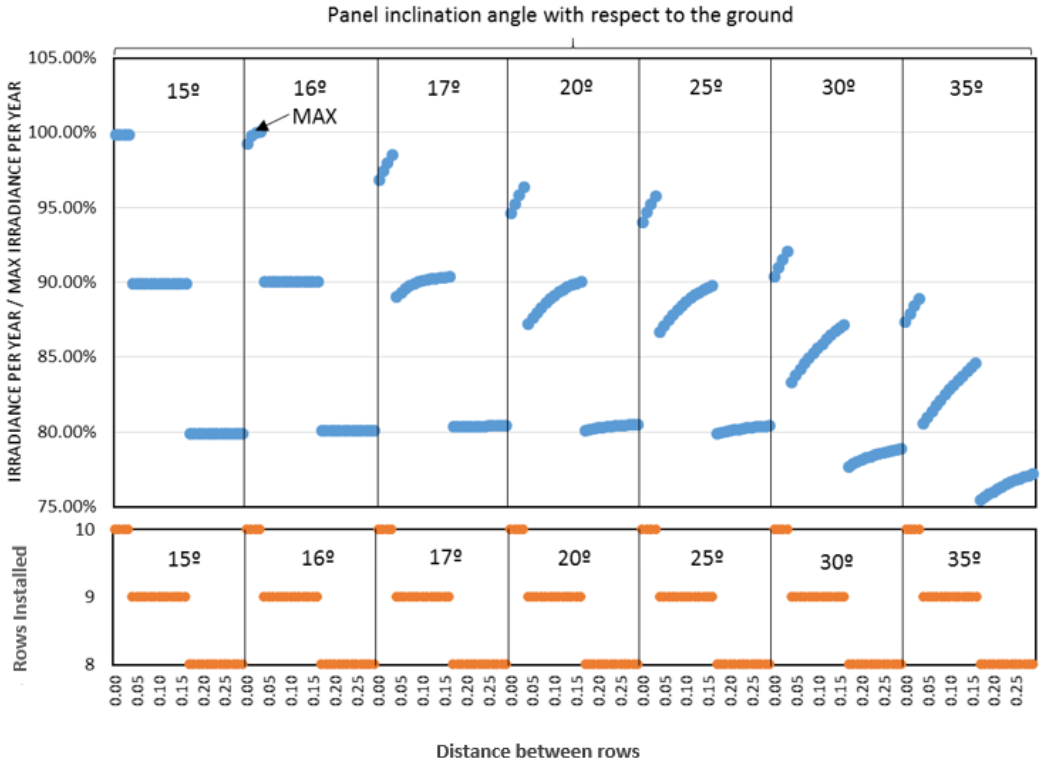

Figure 9. Irradiance on a rooftop solar PV array (roof slope 15°/orientation 180° /latitude 33.7°/10.2x10.2m) for different panel inclinations

Figure 9 shows both the normalized yearly irradiance and number of rows installed versus spacing between rows for a tilt ranging from the flush mount of with the 15° roof to a tilt of 20^{o} respect to the roof or total tilt of 35^{o} from the ground. The maximum irradiance for the constrained area is achieved when tilting 16° with respect to the ground (or a 1^{o} tilt with respect to the roof) and the row distance is 0.04m. The normalized yearly irradiance is taken as the specific yearly divided by the maximum yearly irradiance from all the calculated irradiance results. In this case, the maximum occurred at 16° with a row spacing of 0.04m, and thus it is 100% of maximum solar irradiance. The distance between two adjacent rows (row to row distance) goes from 0 to 0.25 m for all of the panel tilts.

In Figure 9, it is shown that as the row to row distanced increases for array tilt higher than 15°, the irradiance received by the array increases due to decreased shading between panels. Since the design area is limited, the number of module rows decreases with increased spacing, leading to abrupt drops in the irradiance ratio as spacing increases. For an array tilt larger or equal to 17° and a fixed number of rows, increased spacing always yields higher irradiance due to these tilt experiencing significant self-shading when row spacing is small. For all tilt scenarios, increasing distance between rows eventually reduces the number of feasible rows due to the fixed design area. For comparison, when spacing is zero, ten rows can be fit within the design area, while this number drops to eight when spacing increases to 0.15 m. Although not shown, increasing spacing beyond 0.25 m would reduce module rows to seven.

Most importantly, these results indicate the difference in total irradiance when developing a system to maximize solar production for a given design area versus per panel. For the later, the design would yield approximately 80% of the possible energy, as indicated using the 25^{o} tilt system with 0.25 m spacing. At this point, production per panel is maximized. By decreasing panel tilt, self-

shading is reduced, allowing for spacing to be reduced and allowing for an additional two rows of modules.

To further understand how the total irradiance changes due to array tilt, it is important to analyze each irradiance component with various tilt. In Figure 10, the percentage differences in total, direct, and indirect irradiance are presented. All values are presented as the percentage change versus the scenario in which modules are mounted flush with the roof. Since the optimal tilt with respect to the ground is higher than 15º, increasing tilt with respect to the surface will always increase total irradiance until the optimal tilt angle is achieved. At any tilting angles shown in Figure 10, the net beam component is always positive, and the net diffuse component is always negative. Until the optimal tilt is achieved, improved direct irradiance offsets lose to indirect irradiance. Thus the tilting of the array towards local optimal will result in the gain of beam irradiance that is larger than the loss of diffuse irradiance, with the total net irradiance being always positive. The maximum net total irradiance gain is reached when tilting 7° with respect to the 15° pitched surface, or 22° with respect to the ground. Again, the local optimal tilt we obtained for one single module is around 24° when facing 180° at 33.7˚. The reason for the tilting angle to be 22° (2° less than the local optimal angle 24°) is that the net POA total irradiance is regarded as received by the entire array, not a single module. Due to the previous row of panels blocking a portion of the sky, the SVF value of every row in an array is less than that of a single panel at the same tilting angle. The value of SVF is always decreasing as the tilt increases thus the sky-diffuse irradiance is decreasing as the array tilt increases. As a result, the maximum total net irradiance of an array (instead of a single panel) is achieved at 22° and 2° smaller than the local optimal angle for a single panel.

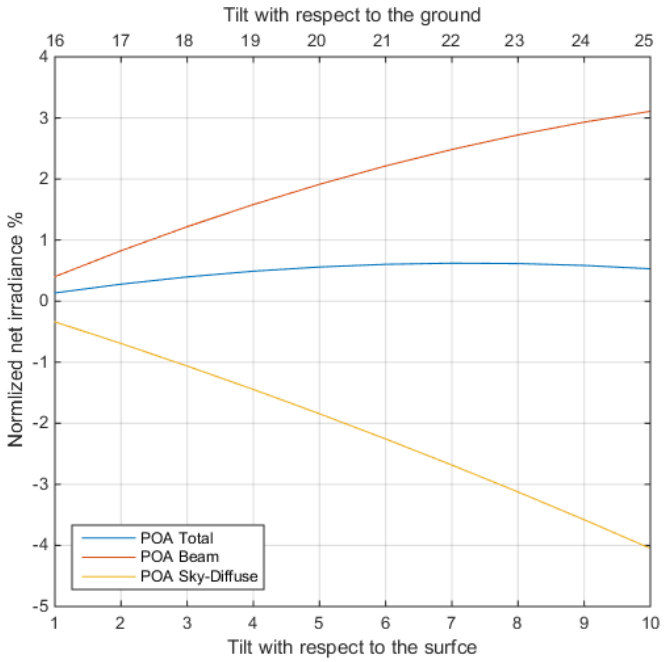

Figure 10. The net irradiance of tilted versus flush array with respect to a surface with 15° pitch, with no shading, facing 180°, with no area constraints

Note that the distance between panels to avoid self-shading depends on the tilting angle, with this distance increasing with the tilting angle. If panel spacing is decreased from this non-shading distance, then panel output will be reduced, but room for additional panels may be created. Figure 11 shows the effect of reducing row spacing from the non-shading distance by up to 0.1 m. For panels with a non-shading distance of less than 0.1 m, the row spacing was reduced up to this non-shading distance, ensuring that panels were not placed under preceding. According to the simulation results, panels with a tilt of greater than 4^o were moved by 0.1 m, while panels with a tilt equal to or less than 4^o were moved by their respective no-shade distances. As shown in Figure 11, moving all arrays forward, for the lower tilting angles shown (1°-4°), the beam irradiance is decreasing indicating the shading loss outweighs the irradiance gain when increasing the tilt of module towards local optimal. At 5°, the gain of beam irradiance is just a bit larger than the shading loss resulting in a net positive percentage value. More importantly, it is due to the fact that start from 5° tilt, the non-shaded distance is large enough so that moving forward by 0.1 m will not

cause the stacking of module, thus the module will not be forced to move to the projection point of the previous row on the surface, thus the shading effect is dramatically reduced. As the tilt increases beyond 5°, the beam irradiance gain starts to outweigh the self-shading loss. However, the sky-diffuse component always decreases, resulting in a negative net total POA irradiance throughout.

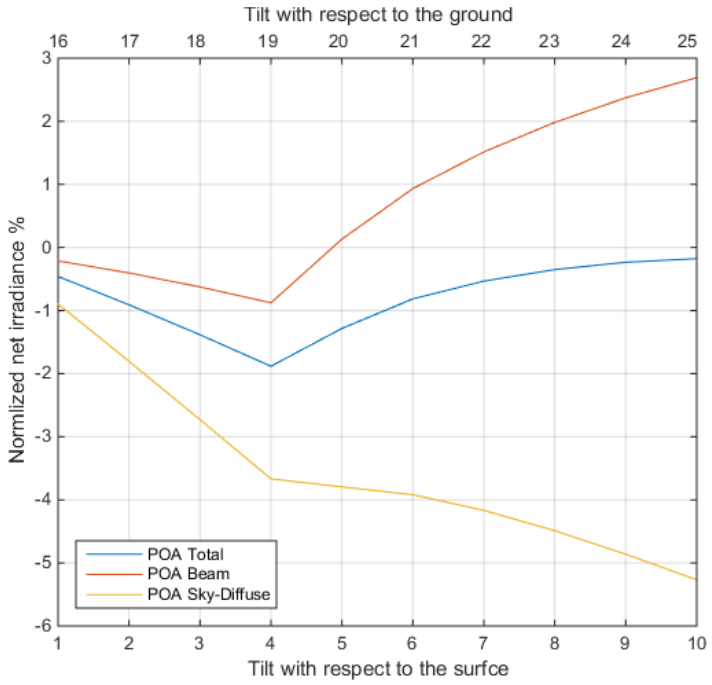

Figure 11. The net irradiance of tilted versus flush array with respect to a surface with 15° pitch, while shaded, by reducing row spacing by 0.1 m, facing 180°, with no area constraint

Increasing the design area from 10.2x10.2m to 10.2x10.88m yields a different optimal angle for maximizing total irradiance, as shown in Figure 6. This particular design area is large enough to allow for increased row spacing, but not to allow for an additional row of panels. Maintaining the same azimuthal and pitch angle as Figure 6 (180^{o} and 15^{o} respectively), normalized irradiance versus row spacing is shown in Figure 12. Having a wider surface allows the larger spacing between rows, thus the shading effect will be minimized and increase the amount of irradiance striking on the modules. Consequently, the array tilt that maximizes irradiance increases from 16°

(shown in Figure 9) to 19° (shown in Figure 12). Since the local optimal array tilt is 22°, the increased roof length allows for rows to separate further apart, allowing higher tilts without causing any shading. Other tilting angles in Figure 12, such as 20° and 25°, are closer to local optimal but receive less irradiance due to shading when row spacing is less available at higher tilting angles.

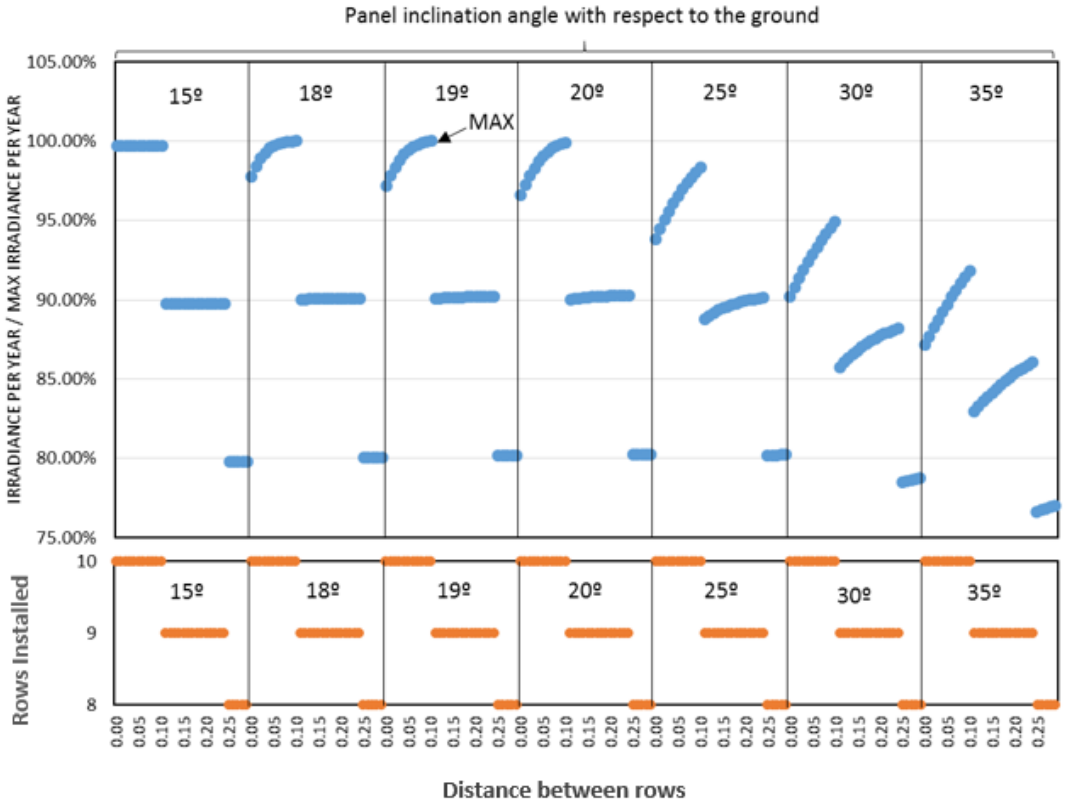

Figure 12. Irradiance on a rooftop solar PV array (roof slope 15°/orientation 180° /latitude 33.7°/10.2x10.88m) for different panel inclinations

In summary, for a surface with a pitch below the optimal tilt angle, maximum total irradiance can be achieved when the row numbers on the surface are maximized and tilted toward the local optimal angle while avoiding self-shading.

These result results have focused on maximizing irradiation when faced with a fixed design area. When typical design goals of maximizing panel output are examined, the MATLAB model yields the same optimal angle as presented in prior work of 24^{o} when panels are spaced to avoid self-shading, as shown in Figure 13. Thus any rooftop PV design to maximize the array output is the

same as maximizing the output of a single panel. Note that these goals are different since the design methodology presented in this work is focused on maximizing output for a constrained design area, versus maximizing output for an individual panel.

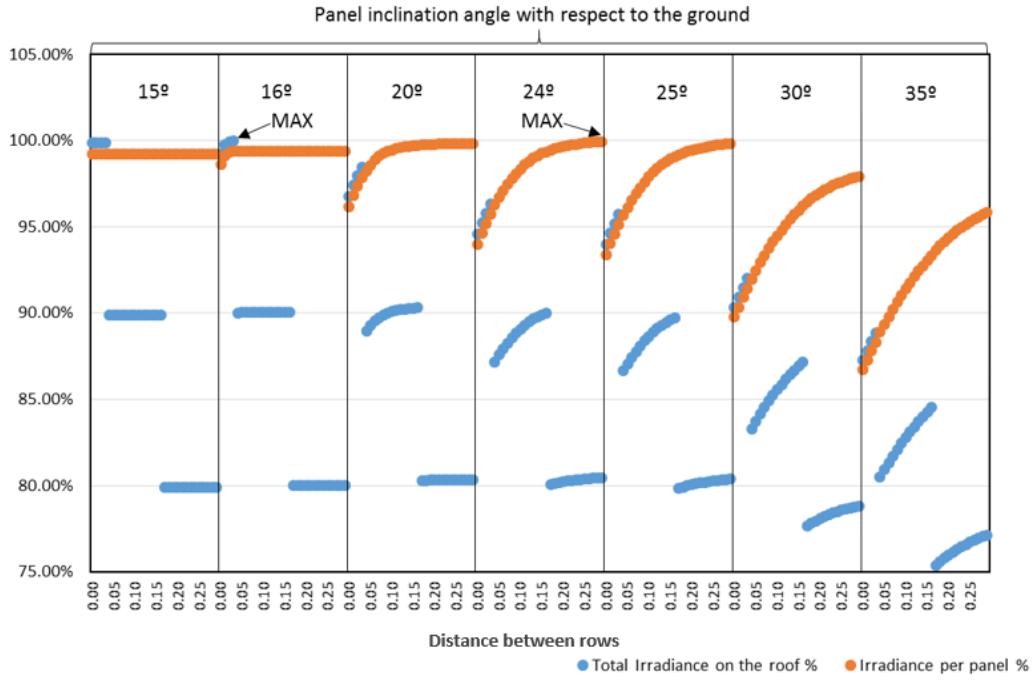

Figure 13. Irradiance received per rooftop PV array v.s. irradiance received per panel

3.2 Irradiance Analysis of a South Facing 30° Pitched Rooftop

For a pitch of 30^{o}, flush-mounted panels exceed the optimal angle of 24^{o}. Increasing tilt will always reduce panel output, as shown in Figure 14. In this instance, panel spacing does not matter since the optimal configuration is flush with the roof. In this instance, maximizing irradiance for a given design area yields the same optimal tilt angle as maximizing individual panel output.

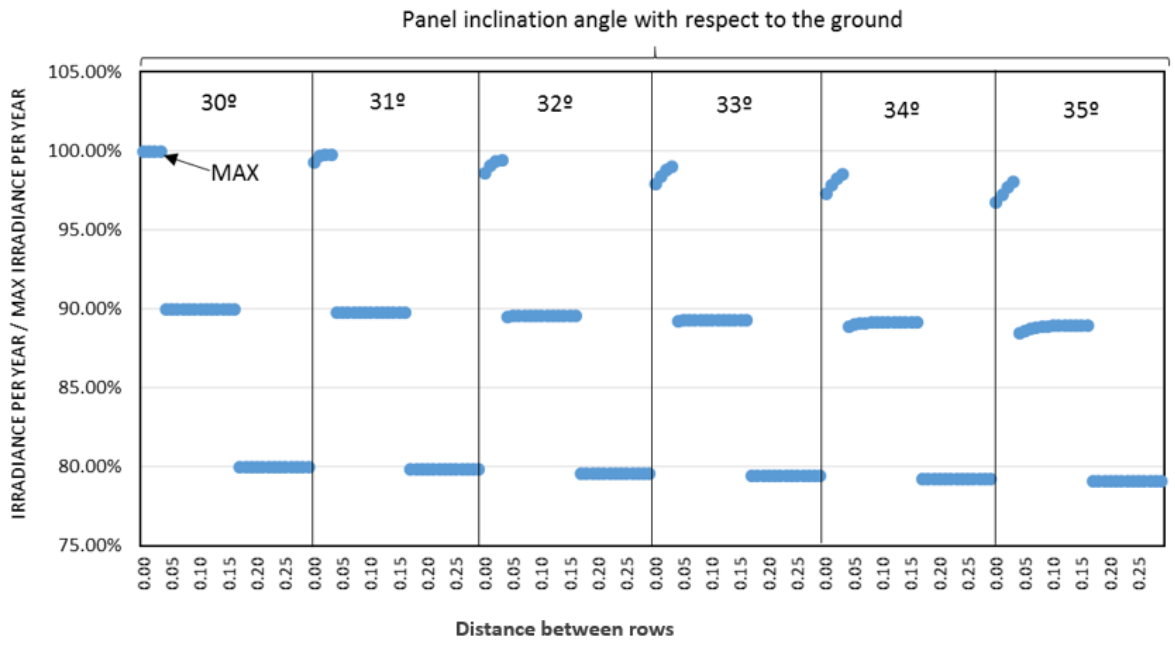

Figure 14. Irradiance on a rooftop solar PV array (roof slope 30°/orientation 180° /latitude 33.7°/10.2x10.2m) for different panel inclinations

3.3 Normalized Irradiance with Various Azimuth Orientation

For two most common rooftop surface tilt such as 15° and 30°, the irradiance received by a single panel lying flat on the two surfaces with various azimuth orientation is calculated and normalized at the same latitude of 33.7˚ N. The irradiance normalization is defined as the irradiance at any azimuthal orientation divided by the maximum irradiance obtained from the azimuthal range 0° to 360°. Figure 15 shows the normalized irradiance versus azimuthal direction when panels are mounted flush (0^o tilt) with the two rooftop surfaces. In Figure 15 the direction of 0^0, 90^0, 180^0, and 270^0 correspond to north, east, south, and west respectively. The normalizing factor is taken as the maximum irradiance for a design area with a pitch of 15^o (subplot (a)) and 30^o (subplot (b)). The maximum irradiance on a surface with a 15° pitch is at an azimuthal angle of 195°, and 197^o for a pitch of 30^o. Figure 15 shows total irradiance, and also the contributions from direct (beam) and diffuse (sky-diffuse),

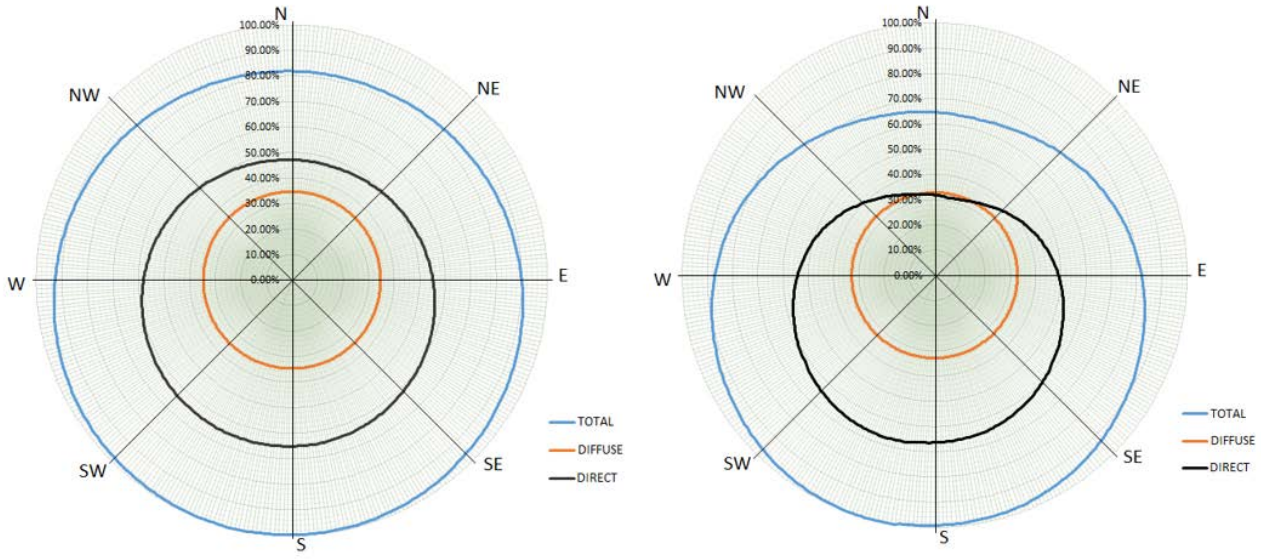

Figure 15. (a) Irradiation on a roof depending upon the azimuthal angle for a roof pitch 15°. (b) Irradiation on a roof depending upon the azimuthal angle for a roof pitch 30° at latitude 33.7°

When compared with the roof surface of 15° to that of 30°, the diffuse irradiance component does not change significantly versus azimuthal angle due to the fact that the variation on SVF is small for two different roof pitch. However, the direct irradiance ratio varies substantially for various azimuthal angle especially at the north (0°). This direction is nearly exactly in the opposite direction of the optimal azimuthal angle. When comparing the two roof pitches with a north orientation, it is noticed at 15^{o} and 30° pitch, the total irradiance at North (0°) is only approximately 80% and 65% of the maximum, respectively. Note that in both cases, the optimal tilt angle is 0^{o}, as shown in Figure 6, and an increase in roof angle yields lower irradiance.

4. Incremental Tilted Solar Array on an Area-Constrained Surface

A novel type of solar PV array layout configuration is proposed here. The solar module in each row is incrementally tilted from the previous row. The tilting angle of the very front row of each array is defined as the initial tilting angle of the PV array. Since the tilting angle of each row is very different, thus the self-shading and blocking effects are different for each row. The analysis of total irradiance on the PV array is not sufficient enough to reflect the electrical energy yield status anymore, due to different shading and blocking patterns from row to row. Thus, the analysis of the electrical DC energy is simulated along with the irradiance.

4.1 Irradiance & DC Energy Yield of Incremental Tilted Array

For incremental tilted array analysis with controlled parameters, several rooftops with various initial tilt (i.e. the tilt angle of the first row in an array) are simulated at the same time to better compare the results. For example, there are seven identical roofs all south-facing (180° from the north) at the location of (33.7°N, 117.9°W). The tilting angle of the very first row of module on the roofs starts varying from 1° to 7° (i.e. the tilting angle of the first row of the first roof is 1° with respect to the roof, that of the first row of the second roof is 2° with respect to the roof, and so on), as the tilting angle of each row of the array (with respect to the ground) has shown in Figure 16.

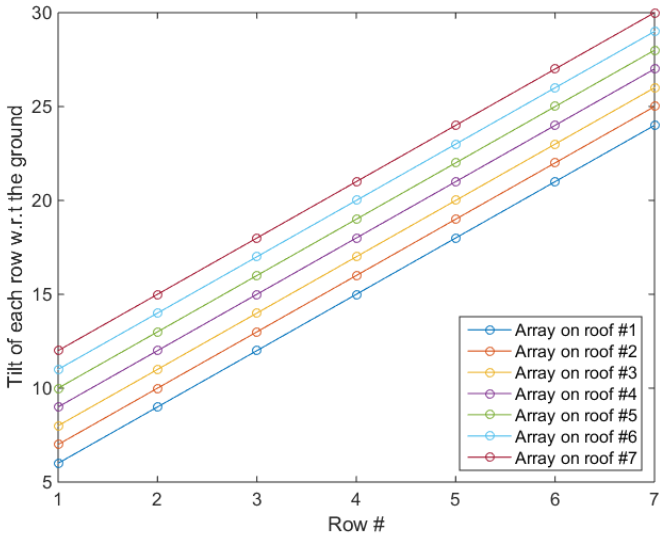

Figure 16. The tilting angle of each row of the 3° incremental titled array on a 5° tilted rooftop with 0% PRDR on the rooftops with respect to the ground

For solar arrays with the GCL-M6/72 355W utilized, those roof surfaces all with 5° tilt, the incremental tilting angle of subsequent rows is 3°. The annual irradiance received by the array, the annual array DC energy from the entire array, and the annual DC energy yield from each row of the module on that roof is all presented as following in three cases. The cases present represent three PRDR values (0%, 20%, and 50%) from the non-shaded row distance.

The string MPPT with all rows connected in parallel for the entire rooftop array is modeled based on the methods used in [37] but specified to the sub-module level shading.

Case 1: 0% PRDR from non-shaded row distance

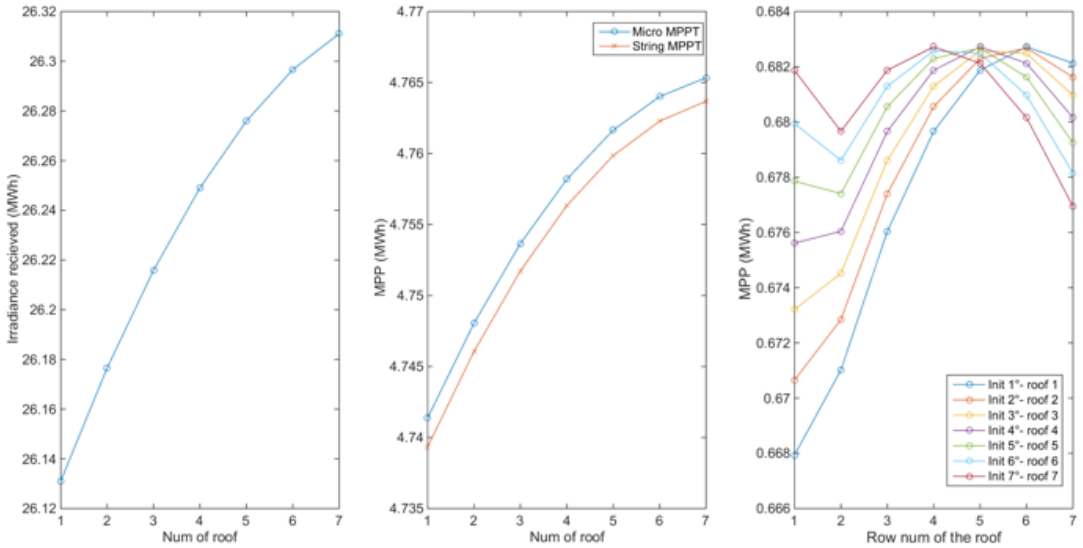

Case 2: 20% PRDR from non-shaded row distance

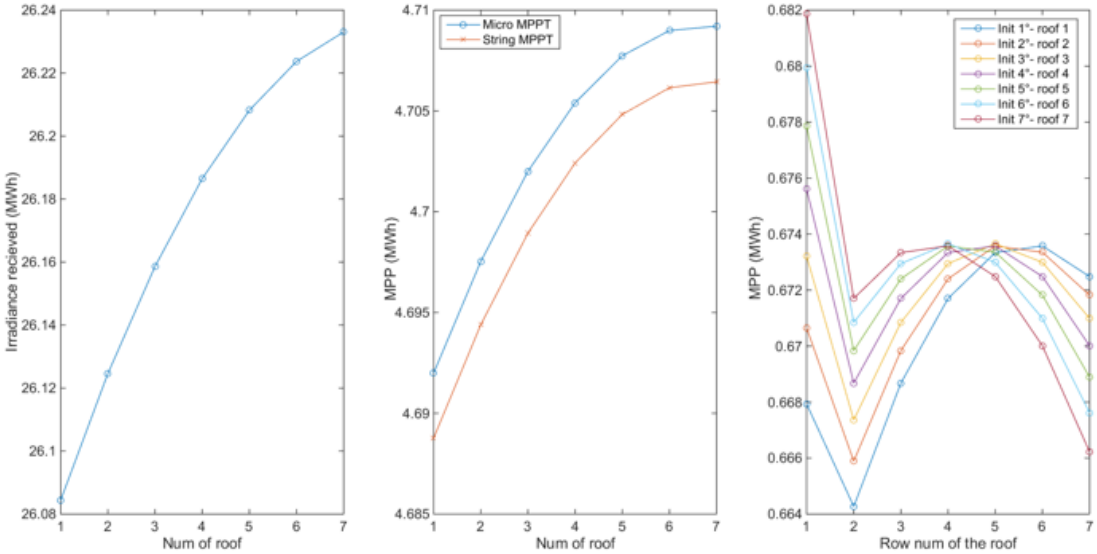

Case 3: 50% PRDR from non-shaded row distance

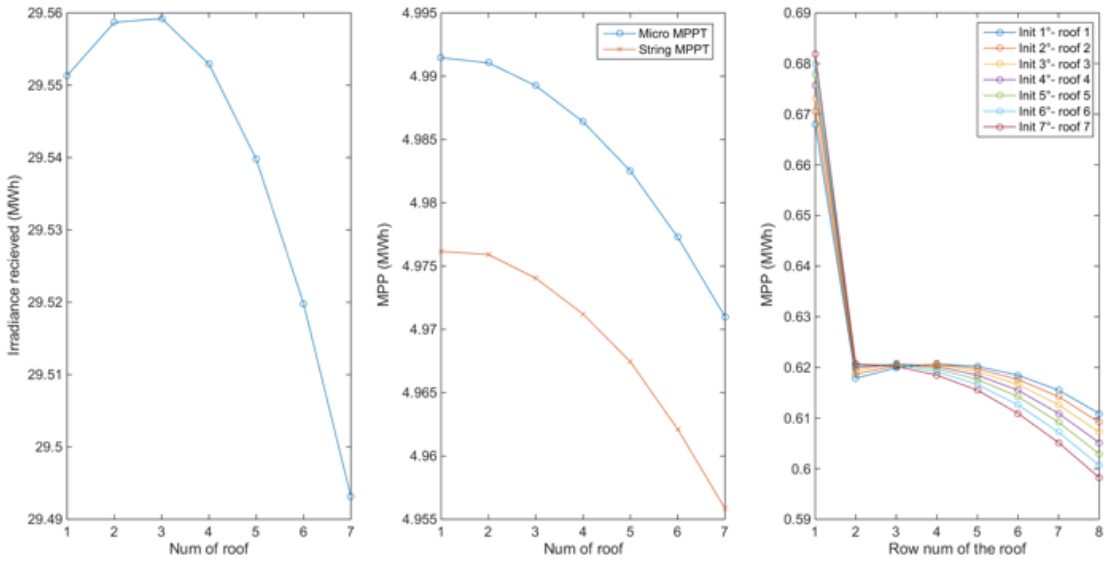

Figure 17. On a 9.5 m long and 5° tilted rooftop, the PV arrays with the incremental tilt of 3° under 0%, 20%, and 50% PRDR, and 7 rows can be installed on every rooftop: (a) The total irradiance received by the arrays with various initial tilting angles; (b) The annual MPP DC produced by the array with module MPPT or string MPPT; (c) The annual MPP tracked by module MPP tracker of each row of the arrays on various south-facing rooftops

From Figure 17 case 1 to case 3, overall the (a) plots suggest the self-shading among rows demonstrate large impact on irradiance received, however, if more rows can be fitted on the rooftop, as DRPR increases, the overall array could potentially receive more irradiance, but the total irradiance received by the individual panel is dramatically reduced. Case 1 (a) and case 2 (a) both indicate as the tilt of the first row of the roofs gradually increases from roof to roof, the array receives more irradiance. However, case 3 (a) shows a reduction trend as the array tilt of the roof increases, the overall received irradiance decreases, which indicates the shading effect is so severe and causes irradiance to reduce more than the gain from tilting the modules higher towards the local optimal.

Among (b) plot in from all three cases, it can be seen, the module-level MPP tracker could track higher DC power than string-level MPP tracker. This is especially true when the shading is most severe, as shown in case 3 (b) compare to almost no shading case in case 1 (b), the module-level

MPP tracker has much better performance under the heavily shaded situation. The trends of DC energy yield curves are similar to the irradiance curve. Even though, the irradiance peaked at roof three in case 3 (a), in the plot (b) the peak is at the first roof instead of the third one. This is caused by the partial shading effect on the panel I-V curve. It is mostly like to be the situation when the most area of the module is under beam irradiation except the corner of the module. In this situation, the modules receive most of the irradiance that striking on the module surface, but almost lost 1/3 of the power output due to the shaded corner.

In case 1 (c), at the 0%, the differences in energy received of the first rows among all 7 roofs are larger than the differences of the back rows among roofs, and this is due to the blocking effect from pervious row and small amount of shading effect at early morning and late evening offsets the power production gain from higher module tilts. It is noticed, in row 5, the energy production from row 5 in roof 7 is no longer the highest among other roofs, which indicates when blocking effect and self-shading took place, tilting the module higher toward local optimal would not help yield more energy under the incremental tilted scenario. Case 2 (c) demonstrates that under 20% PRDR while comparing the transition from 1^{st} to the 2^{nd} row among roofs, it is noticed, the second row always produces less energy compared with the first row, and roof seven which has the highest tilting angle, to begin with, has shown the biggest drop from row one to row two, which indicate shading and blocking effect has bigger impact on higher tilting rows than the lower tilting ones. However, case 2 (b) demonstrates the energy summation of all the rows of roof seven is the highest among all other roof arrays. Thus, even though the energy production from each row of a high tilting array drops much quicker than that of the low tilting array, the overall array production is still the highest when the PRDR is kept at a low value (in this case 20%). Lastly, it is worth to point out that in case 2 (c), as the PRDR becomes 50%, roof 7 is no longer the highest yield row

starting at row 3 (this value was row 6 in case 1 and row 5 in case 2), and this directly resulted in the overall energy production from low tilting array (roof one) to be the higher yield rooftop. However, because of the high PRDR value (50%), an additional row of the module can be fitted on the roof, this increases the overall roof production with constrained area.

5. Comparative Analysis of Incremental & Constant Tilted Array

Both constant tilt and incremental tilted array have been simulated and analyzed in detail in previous sections. The comparative study is performed in this section to comprehensively investigate the difference of energy yield performance and module economics between incremental tilted and constant tilted layout.

5.1 Array Performance under Various Shading Conditions

For the 5° tilted south-facing rooftop having the same dimensions as the three cases above, with 0% to 50% row space reduction from the non-shaded distance (0% DRPR), both incremental and constant (constant tilting angle other than flush mount) tilted layout with maximum array DC energy output normalized by the energy yield of the flush-mounted array are plotted in Figure 18. From model output results from 1° to 5° increment, it is found that a 3° increment can achieve the best panel economics. In Figure 18, at each PRDR point, multiple rooftops with various value of initial tilt (the tilt of the very front row on each roof) with 3° increment are calculated, and then the array that produces maximum DC energy is saved as a data point and then normalized by the energy output of the flush-mounted array and then plotted in Figure 18 at that DRPR value.

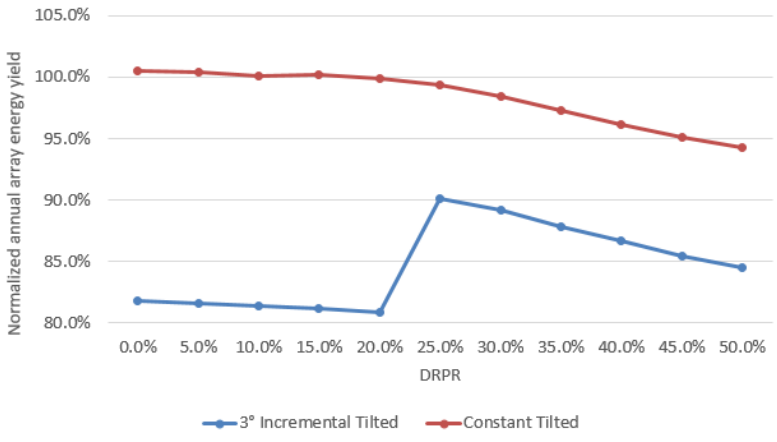

Figure 18. The normalized annual array energy production of constant and 3° incremental tilted array by the flush-mounted array at various PRDR on a 10.9m length 5° pitched south-facing rooftop

It can be seen that the constant tilt layout yield slightly better than flush-mounted array on the roof, as the PRDR increase, the array energy from both increment and constant tilted array decreases comparing with that of the flush-mounted array as DRPR increases. The sudden jump of increment tilted array as PRDR increases from 20% to 25% due to additional row added on the roof surface. As the PRDR increases from 25% to 50%, the sub-module shading gradually increases, the energy production from the array is decreased dramatically. For the 3° incremental tilted array, after the jump, it remains 10% to 15% less compare with the flush mount because it still can install one less row of the module as well as the effect of shading.

The total production of energy from the solar array is certainly important. However, in Figure 19 panel economics which indicates the energy produced per panel throughout a year is also crucial in terms of project financial and payback analysis. The measurement of panel economics is made against the flush mount array as it has been the most common installation layout option. In Figure 19, as 0% PRDR, the panel economics is better for both the constant tilt and incremental tilted array, as the shading progresses, the economics dropped sharply comparing.

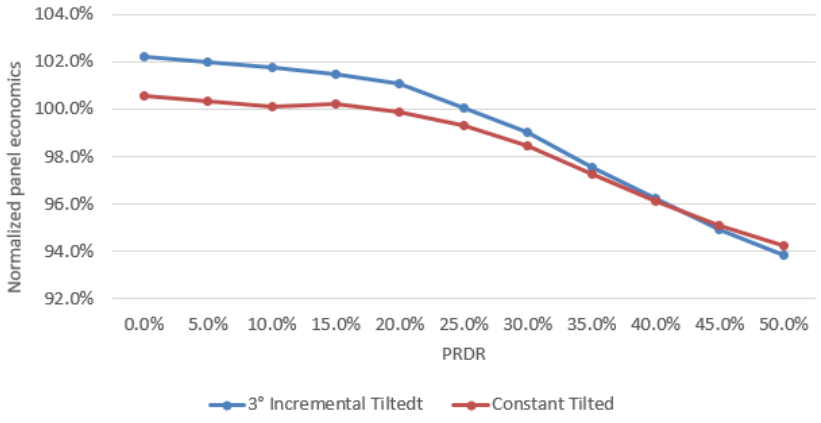

Figure 19. The normalized annual array panel economics of constant and 3° incremental tilted array by the flush-mounted array at various PRDR on a 10.9m length 5° pitched south-facing rooftop

Figure 20 shows the normalized irradiance received by both the incremental tilted and constant tilted array is relatively constant. The constant tilted line represented the irradiance does not change much and the incremental tilt remains roughly constant. Refer back to Figure 18, it can be seen that even the array may receive the equivalently amount of irradiance but the partial shading effect on the energy production could be significantly reduced as shading progresses.

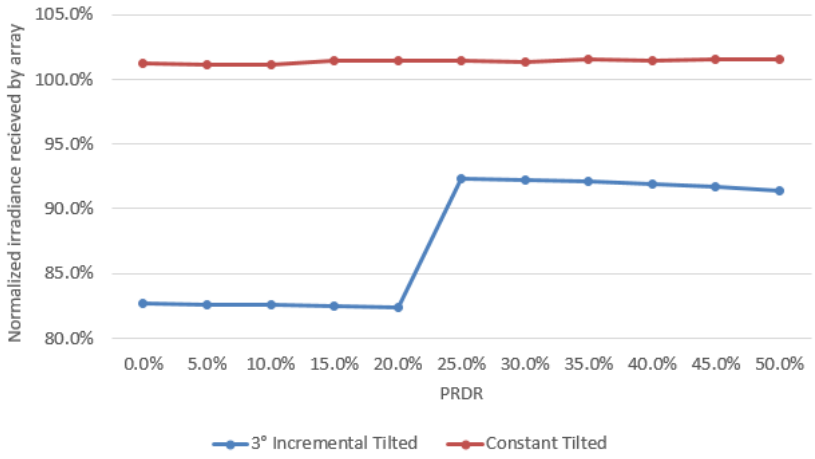

Figure 20. The normalized annual array received irradiance of constant and 3° incremental tilted array by the flush-mounted array at various PRDR on a 10.9m length 5° pitched south-facing rooftop

As the PRDR increases, the panel economics normalized against flush mount are gradually moving towards negative. Even the incremental tilt produces less energy but the panel economics has been better than both the flush-mounted array and the constantly tilted array layout.

5.2 Array Performance with Various Roof Pitches

To better understand the array energy yield, irradiance, and panel economics on various rooftop tilting angles ranging from 0° to 30° under 30% PRDR are plotted in Figure 21.

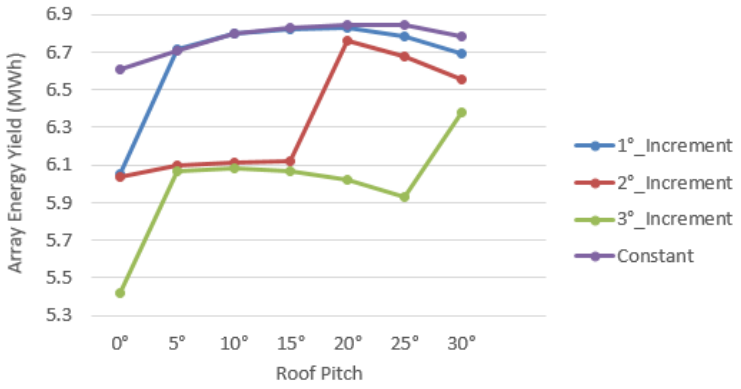

Figure 21. Annual array energy produced by incremental and constant tilted array at various south-facing rooftop pitches under 30% PRDR

Shown in Figure 21, as the tilting angle of the rooftop increases, the array energy generally increases and quickly decreases as the roof pitch becomes higher. The jumps of array energy are due to the additional row of modules added on the roof surface. Also, as the incremental angle increases from 1° to 3°, the array energy yield reduced at each roof pitch. Overall, under PRDR of 30%, it is seen the constant tilted array has the best performance with the highest DC energy output. From the irradiance perspective shown in Figure 22, the irradiance profile matches that of the array energy output.

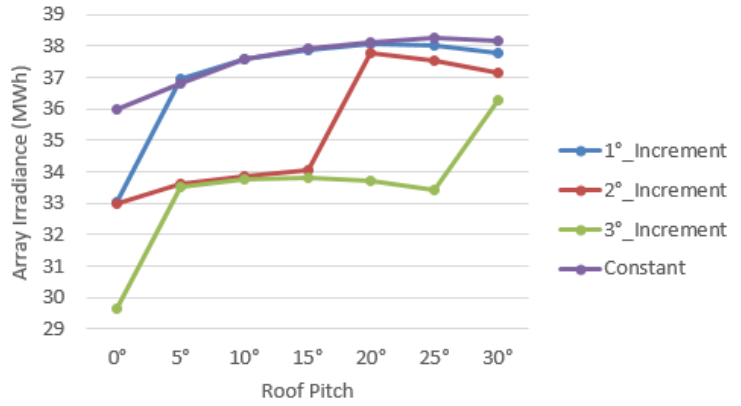

Figure 22. Annual irradiance received by the incremental and constant tilted array at various south-facing rooftop pitches under 30% PRDR

However, the panel economics under PRDR of 30% as shown in Figure 23 indicates at a lower roof pitch, the panel economics showing higher values comparing with constant tilt. In fact, the

high incremental tilting angles at lower roof pitches present better panel economics compare with 1° and 2° increment tilt. However, as soon as the roof pitch reaches 10°, the lower incremental tilting values out-performed the 3° incremental array. The constant tilting array at high roof pitches (above 10°) shows better panel economic performance than all the incremental tilting array as shown in Figure 23.

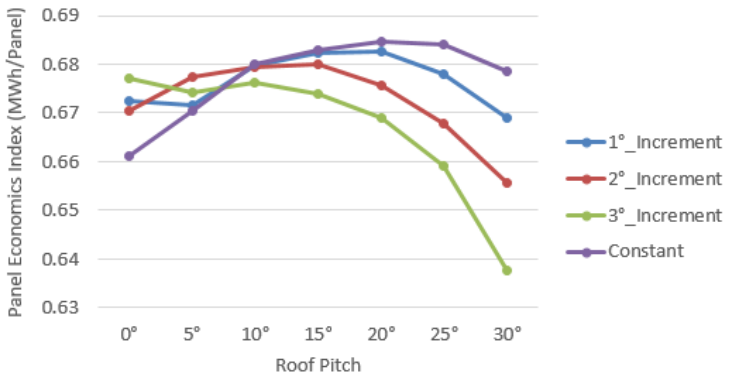

Figure 23. Panel economics from the incremental and constant tilted array at various south-facing rooftop pitches under 30% PRDR

It is also noted in Figure 23 that as the roof pitch increases, the panel economics of high incremental tilted array dramatically reduced.

From the results and analysis above, the constant tilt layout demonstrates high energy production through various roof pitches and relatively good panel economics only at high roof pitches under 30% PRDR. Thus, for a solar project focused on rapid payback with low roof pitches, it is more desirable to choose an incremental tilting layout.

5.3 The 1° Incremental & Constant Tilted Array

From previous results and analysis, the 1° incremental tilted array has the best energy yield and array economics among other incremental tilted values. Thus, this section specifically focuses on the 1° incremental and constant tilted PV array. From Figure 21 to Figure 23, it is noted that the constant and the 1° incremental tilted array performs better on energy production and panel

economics in higher roof pitches under 30% PRDR partial shading and blocking condition. Thus, both of the layouts are selected under various PRDR on roofs with different pitches to see how the array energy yield and panel economics would change at both light and severe shading and blocking situations.

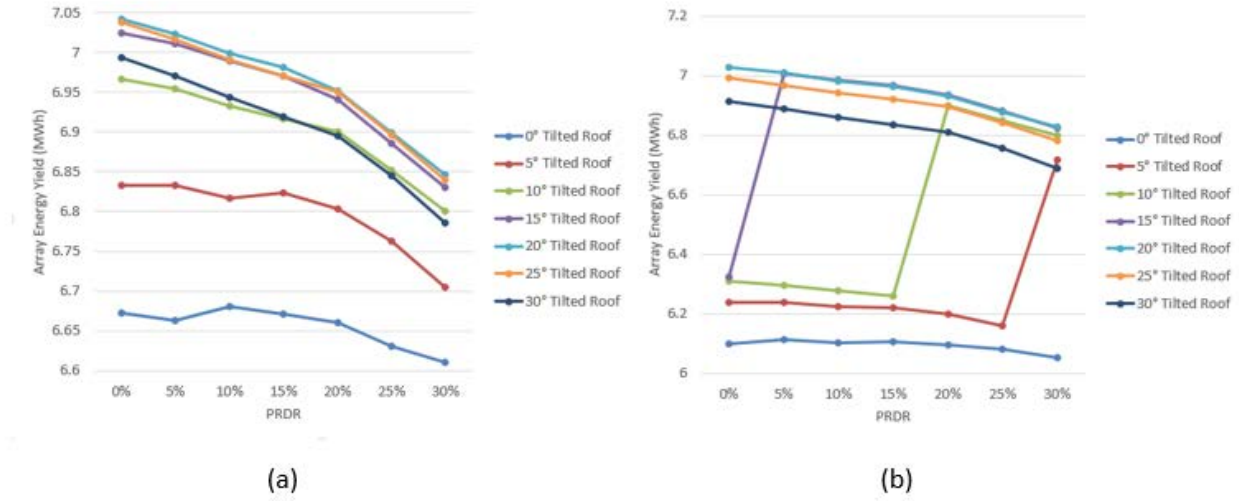

Figure 24. Annual energy yield of constant and 1° incremental tilted array on various south-facing rooftop pitches at different PRDR

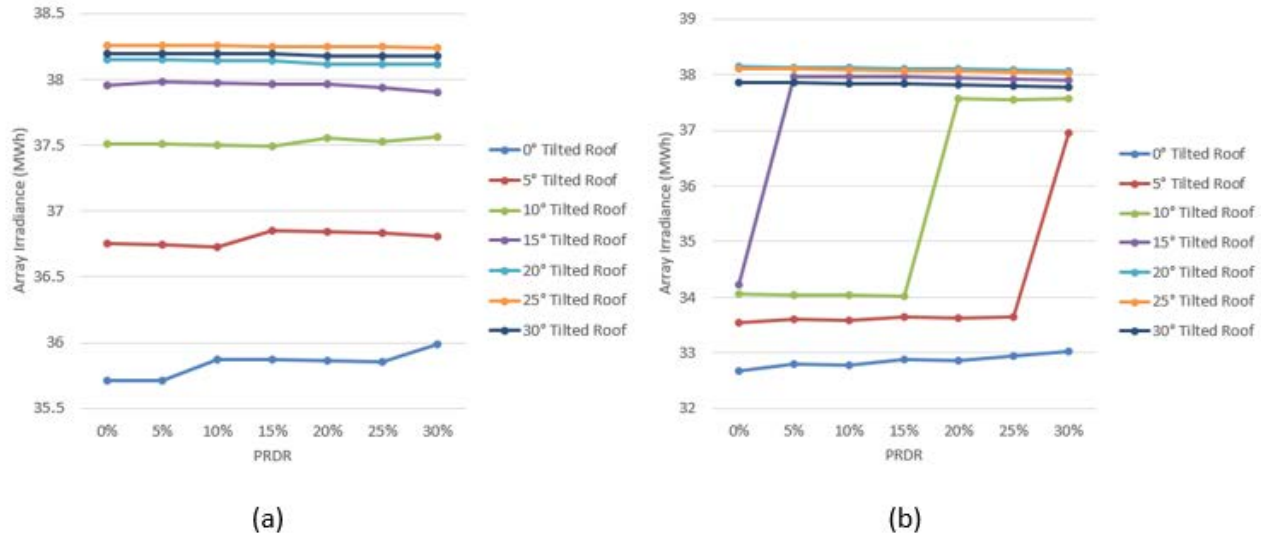

Figure 25. Annual irradiance received by the constant and 1° incremental tilted array on various south-facing rooftop pitches at different PRDR

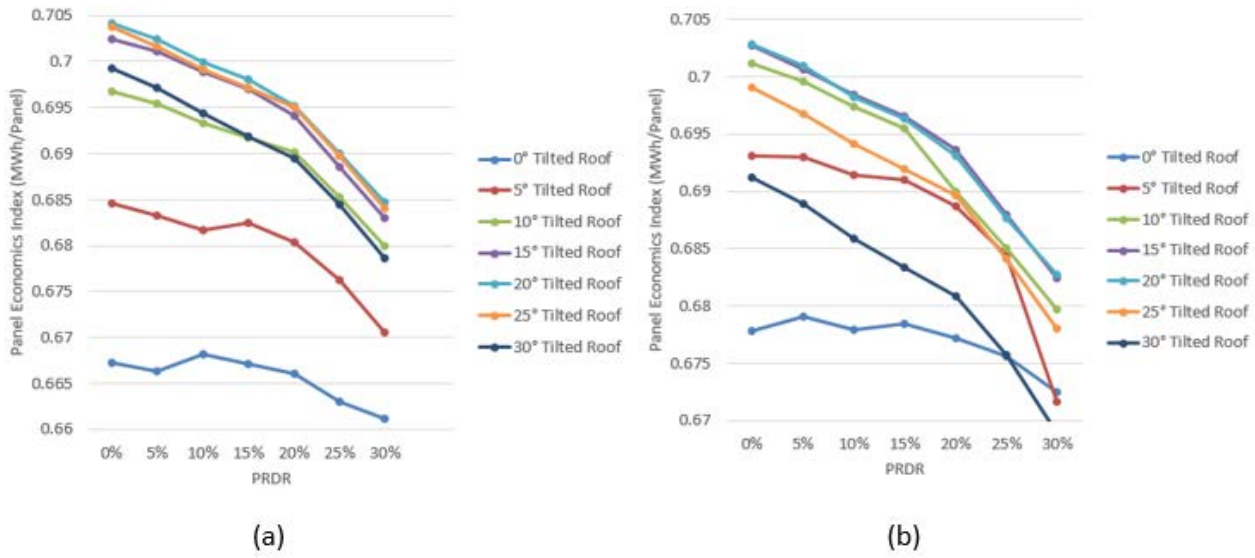

Figure 26. Panel economics of constant and 1° incremental tilted array on various south-facing rooftop pitches at different PRDR

In Figure 24 (a), the array energy produced generally decreases as the PRDR increases. As the rooftop pitch increases from 0° to 20°, the energy production has increased dramatically at each PRDR. The line that corresponds to the 20° tilted roof pitch is the highest energy production among all other roof pitches in Figure 24 (a). The 25° roof pitch shows a lower energy production than the 20°, and that of the 30° pitched line shows even smaller production and the energy produced almost equivalent to that of the 10° pitch. Also, the "bump" of the energy yield of the array on the same pitched roof is caused by the tilting angle of an array at each PRDR is different. For example, for 0° pitched rooftop, at 0% and 5% the tilt of array yields maximum energy is 2°; from 10% to 25%, the tilt of array yields maximum energy are all 3°; however, at 30%, the tilt yield maximum energy is 4°. From Figure 24 (b), the general trends of the arrays at increasing PRDR, the energy produced by arrays are decreasing. The jumps occurred at each PRDR for three of the five pitched rooftop, indicated as the row to row distance reduced, additional rows of the module can be added, and thus the array produces more energy. For the 0° pitched roof, when the PRDR at 0% the array that produces maximum energy is tilted from 2°-10°; at 5% and 10%, the maximum energy array

is tilted from 3°-11°; at 15%, the maximum energy array is tilted from 4°-12°. Therefore, for a particular rooftop as the PRDR increases, the module energy may vary.

Interestingly, Figure 25 shows the total array irradiance received by those same arrays. It is surprising to observe the irradiance at increasing values of PRDR for each tilted roof is also increases. At 0%, for different roof pitches, the total irradiance ranges from 35.7 to 38.3 MWh and the total energy ranges from 6.67 to 7.04 MWh. However, the array energy instead decreases due to partial shading. The shading and blocking effect at the same PRDR for various roof pitch does not affect much in terms of irradiance received, but the effect on the I-V and V-P curve for each module is significant since a slight shading on one cell could block the energy from one of the sub-module thus causing the notable difference on module's energy production. In Figure 25 (b), for lower pitched roofs such as 0° at high PRDR values, the array irradiance even increased. However, at higher roof pitches, the array irradiance remains roughly the same.

From Figure 26 (a), the trends of panel economics affected by shading and blocking at various PRDR can be clearly seen and are similar to the profile of array energy yield, since the number of rows of the module can be placed on the roof surface are the same. In Figure 26 (b), the panel economics of 0° and 30° pitched rooftop appears to be the worst among other roof pitches. The 15° and 20° pitched roof demonstrate the best panel economics, due to the fact that the incremental tilt could bring the modules close to the range of local optimal tilt. Thus the irradiance received by each module of the incremental tilted array does not vary too much. It can also be pointed out that the sudden drop of panel economics at 30% PRDR is due to an additional row of the module that can be installed and the rows are under server shading condition.

To better compare the results of energy yield and panel economics between the two, it is necessary to obtain the normalized results of the 1° incremental tilted array by the constant tilted array as shown in Figure 27 and Figure 28.

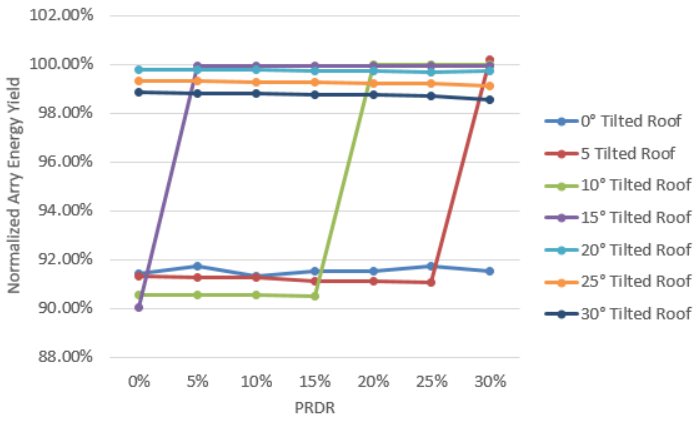

Figure 27. Array energy yield of the 1° incremental tilted arrays is normalized by that of the constant tilted arrays on various south-facing rooftop pitches at different PRDR

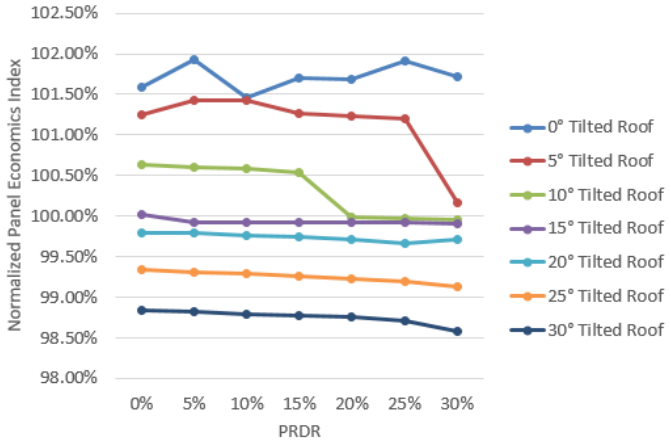

Figure 28. Panel economics of the 1° incremental tilted arrays is normalized by that of the constant tilted arrays on various south-facing rooftop pitches at different PRDR

From Figure 27 it can be seen, the energy yield of 1° incremental tilted array on high pitched rooftops such as 20°, 25°, and 30° is close to but all slightly smaller than the energy yield from constant tilted arrays under all PRDR values ranging from 0% to 30%. From Figure 28, the panel economics of the 1° incremental tilted array on a flat rooftop is almost 2% better compare with that of the constant tilted array at 5% PRDR. Also, the lower-pitched rooftops such as 0°, 5°, and

10° appear to be generally better in terms of panel economics than the constant tilted array under PRDR values ranging from 0% to 30%.

6. Rooftop Solar Modeling & Design with Commercial Software

Many residential and commercial rooftop based solar PV system is designed by sophisticated commercial software. In the past, due to the nature of rooftop solar design, the site visit is usually necessary to understand the physical conditions of the rooftop, such the height of obstruction and the rooftop orientations, before any design is made. Nowadays, many software has integrated their simulation interface with satellite images such as Google Map to help the designers to make a better decision if they can observe the rooftop conditions without any physical presence onsite. In this section, the method of designing a rooftop solar PV system with best practices using existing commercial software is introduced and analyzed in detail with examples. At the end of this section, the design & planning methodology applied to an urban community consisted of residential, commercial, and industrial sectors. This urban community is located at Oak View, Huntington Beach, California. Three possible scenarios of such an urban community are presented, each with a different constraint for the amount of solar PV capacity that can be installed in the community.

6.1 General Rooftop PV System Design Procedures

After the rooftop site location has been identified on Google Maps, the detailed design procedure is conducted in order to more precisely estimate the PV system size and performance. When designing a solar PV system, the visualization is crucial to understanding the rooftop condition and installation potential. Thus usually the field commissioning should be conducted prior to the system design phase, however, for a large community consisting of hundreds of buildings, such a process may not be the most practical nor efficient. Thus, an alternative approach is using a satellite image-based graphical interface software to help construct a rooftop PV system layout in a more visually appealing manner. By introducing the map-based graphical interface PV design tool, the designer is able to quickly identify the roof structure and the locations of the obstacles thus make

a rational decision on the possible PV array layout configuration. In this section, the commercial software Helioscope is used to conduct the demonstration of rooftop solar modeling.

6.1.1 Step 1: Outlining the Shape of Rooftop

PV system design on a software starts from drawing the roof structure and outline to generate 3D buildings as shown in Figure 29. Some information about the roof is needed, such as the tilt and azimuth angle of each roof piece.

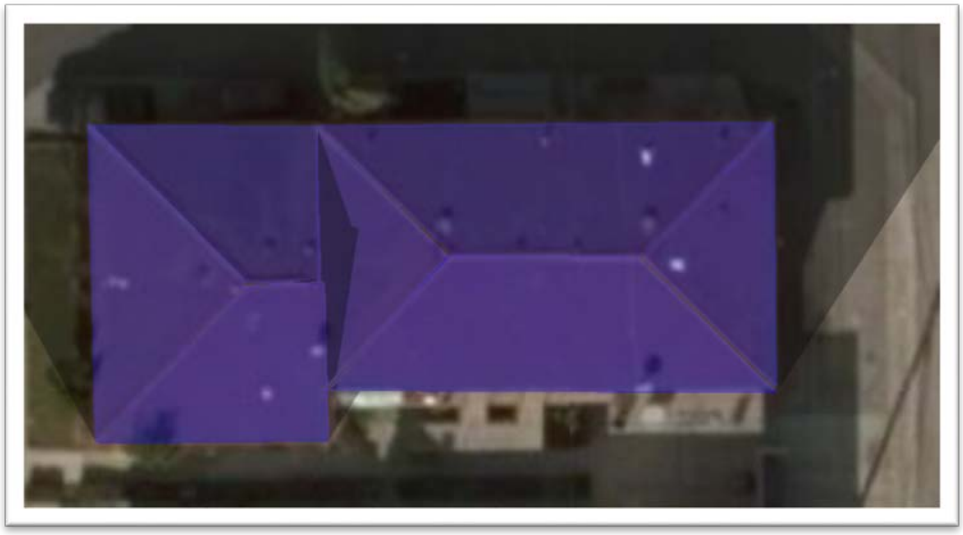

Figure 29. Outline the rooftop and the generated 3D structure

The environmental obstacles such as trees, HVAC, ventilation systems, and even utility poles can be outlined as well as shown in Figure 30, so the shading from those obstructions can be automatically generated to avoid PV module layout.

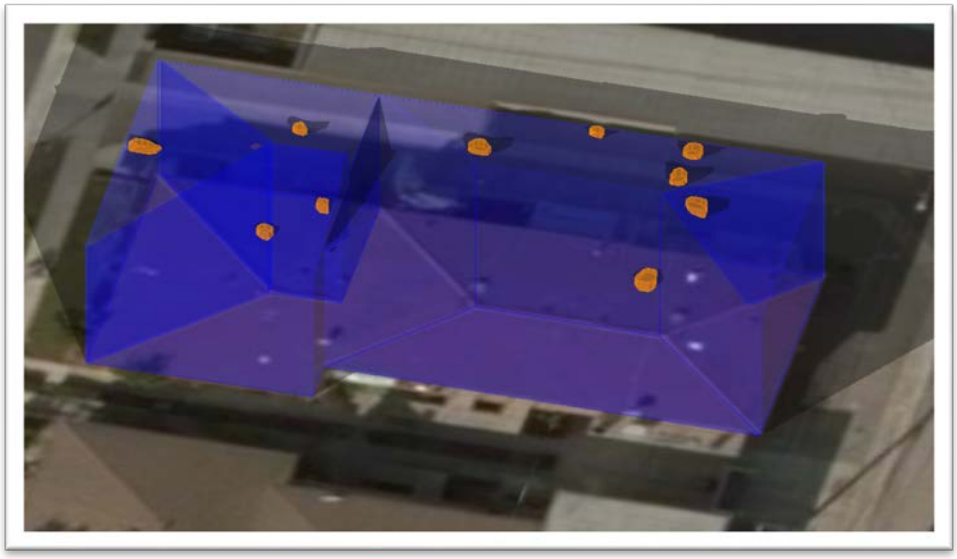

Figure 30. Drawing out and the generated 3D obstructions on the rooftop

6.1.2 Step 2: Solar Module Placement & Setback Rules

After the shape of the roof is drawn and the obstructions are identified, the setback rules from the local & state fire department and Division of State Architect for the installation of a rooftop PV system must be addressed for commercial & industrial (C&I), residential, and carport PV systems. According to the California Department of Forestry and Fire Protection Office of the State Fire Marshal, the rooftop access, pathways, and smoke ventilation all have restrictions [38]. For example, a residential building with hip roof layouts, the modules should be located in a manner that provides one three-foot-wide clear access pathway from the eave to the ridge on each roof slope where modules are located shown in Figure 31. The rules may vary depending on the roof types.

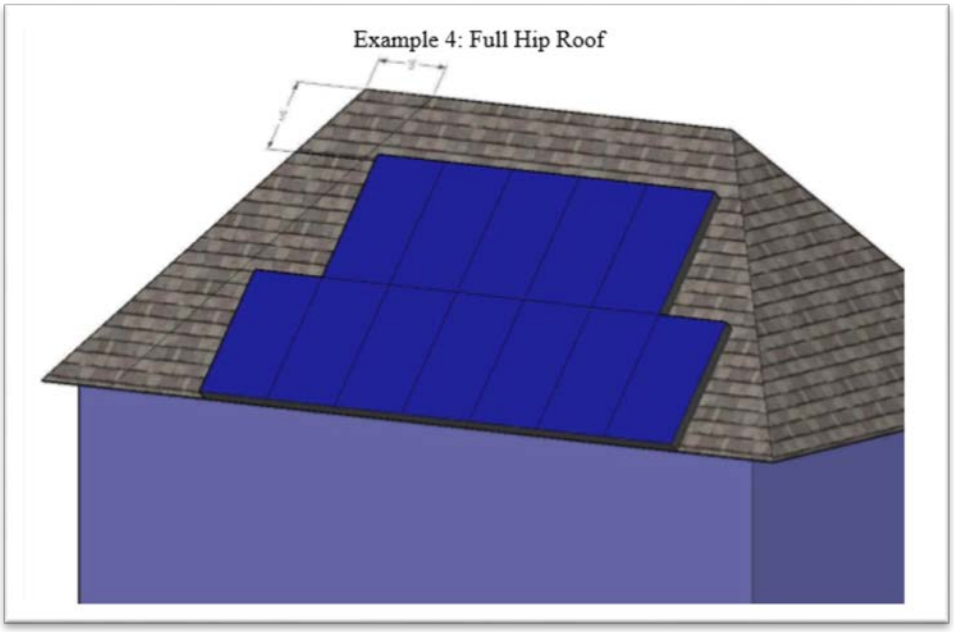

Figure 31. A sample solar PV array layout and design setbacks requirement from the California Fire Department [38]

The solar array on the rooftop without setback has been generated based on the available spaces shown in Figure 32. The effect of applying design rules from the fire department could decrease solar installation potential. Figure 33 below shows there are only 26 pieces of solar modules when applying the fire setbacks, but for Figure 32, without and setbacks there used to be 46 pieces of solar modules on the same rooftop. There is a relatively large reduction from 26 to 46 for an individual house. When working on any PV project, it is important to understand the design rules and requirements from the local fire department and building code. For commercial building and carport PV array layout, other rules may apply.

Figure 32. Rooftop with solar PV array that has zero feet setback from the edges

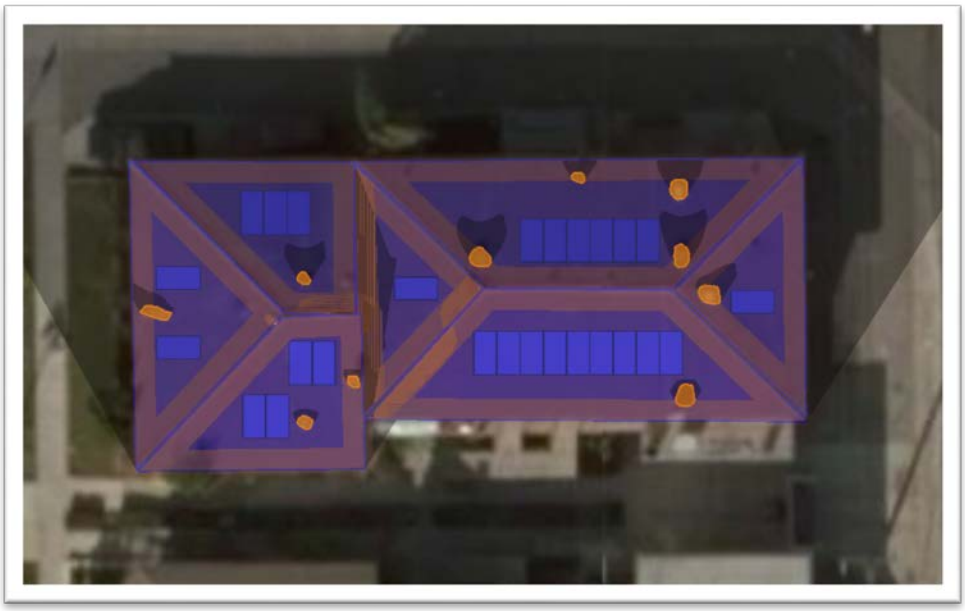

Figure 33. Rooftop with solar PV array that has 3 feet setback from the rooftop edges

6.1.3 Step 3: Solar Irradiance Estimation

After setting up a fire lane, setback, and walkway of the rooftop PV arrays, the next step is to identify the rooftop solar irradiance intensity distribution for a rooftop structure. As shown in

Figure 34, the brightest region indicates the highest solar irradiation which is usually the north-facing surfaces. Sometimes, the rooftop top surface could have self-shading on top of each other. The south-facing lower rooftop surface presents the darker region at the intersection with the taller surface on the right. Therefore, such an irradiance indicator demonstrates the possibility for the designer to imminently identify the regions on the rooftop that is best for the PV array installation.

Figure 34. The annual sun irradiance distribution on the rooftop [39]

After understanding the solar irradiance distribution on the rooftop, there is still a need to estimate the shading effect caused by the obstruction on the solar modules and determine the intensity of shading on each individual panel. The optimal module placement location can be decided in Figure 35. From Figure 35 below, the red-colored solar panel has the most server shading caused by the obstructions nearby. Based on the irradiance distribution in Figure 34 above, the red solar panel and the panels placed on the north-facing rooftop should probably be removed.

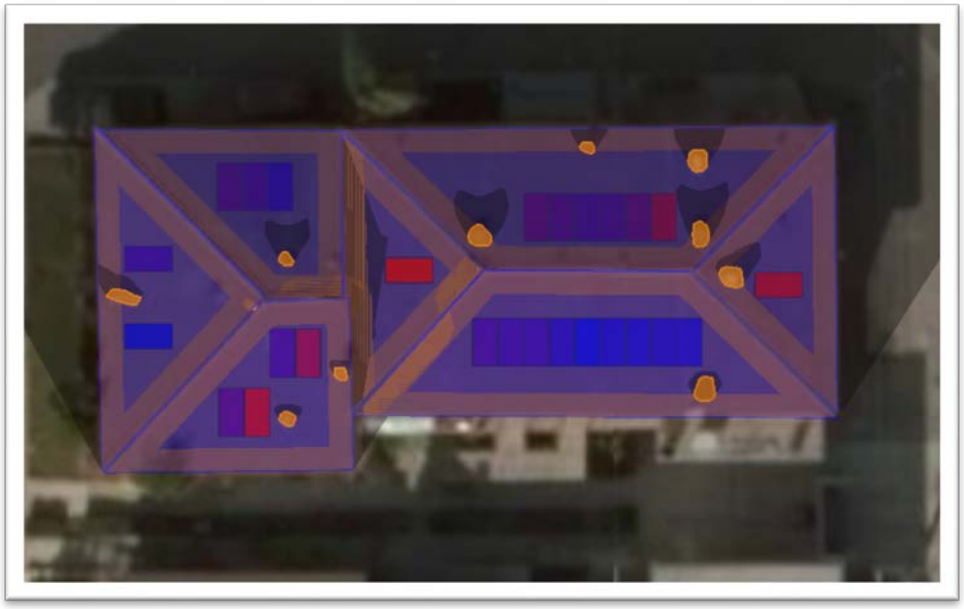

Figure 35. Rooftop solar PV module shading condition caused by the nearby obstructions

6.1.4 Step 4: Inverter & Wiring

After the modules are well placed on each rooftop surface, the sizing of the electrical components will then be addressed. Both power and voltage need to be considered when sizing the inverter. Usually, the optimal DC/AC ration would be from 1.1 to 1.25, depending on the region and solar irradiance. For community and district level solar PV systems to prevent clipping loss (when the DC input exceeds the inverter's conversion limits), different types of inverters should be considered. String inverter would be most practical when designing a solar PV system on residential buildings because there are the modules usually placed on multiple roofs with different azimuth orientation, therefore for the sun at a certain position, the POA irradiance on each roof surface would be different thus interference the production of solar modules on those surfaces, unless the inverter is equipped with multiple MPP trackers. From the energy yield perspective, in the residential sector, both the micro-inverter and sting inverter with multi-MPPT could help to lower the impact of the mismatch loss of the array.

Figure 36 shows this roof placed with solar panels in every roof facing orientation with only one inverter having a DC/AC ration of 1.04. Notably, this system has a Mismatch loss of 10.7%, with an overall performance of 69.9% shown in Figure 37.

Figure 36. The multi-orientation solar PV array on a tilted rooftop connecting with one inverter

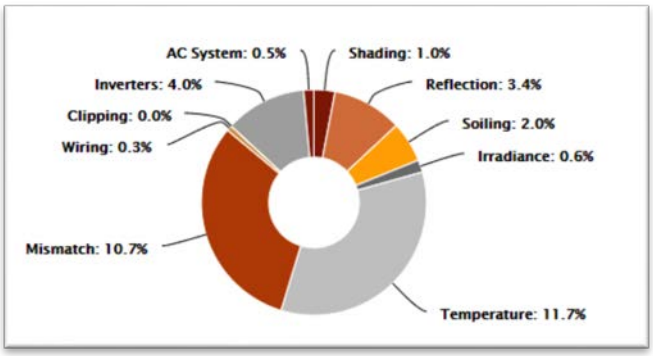

Figure 37. The PV system loss chart of the multi-orientation array with one inverter

When having four inverters with 2kWp each shown in Figure 38, the Mismatch loss is reduced to 5.1% which is a relatively lower loss, with a performance ratio of 74.4% shown in Figure 39. Thus, for a community project, from an energy production efficiency perspective, it is mostly desired to

place a solar panel on the south-facing side or using string inverter with multi-MPPT for various orientations to avoid high mismatch loss.

Figure 38. The multi-orientation solar PV array on a tilted rooftop connecting with four inverters

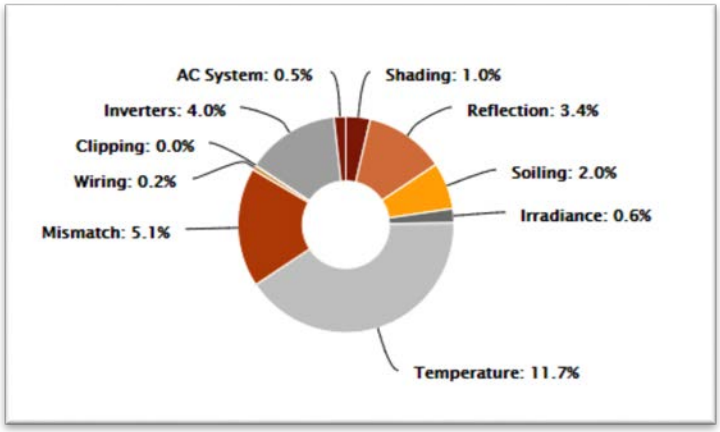

Figure 39. The PV system loss chart of the multi-orientation array with four inverters

From the O&M perspective, string inverter would also lower the O&M cost and usually ideal for limited space on the rooftop. For large C&I and parking lot solar PV system, the central inverter would be the best choice in terms of lower cost per unit of watt, fewer connections between components, and easier for installation or replacement [18]. For large C&I and parking lot PV arrays setting up wiring zone is necessary sometimes when two or more structures with PV arrays

that are located closely. Setting up a shared wiring zone would also help reduce the number of AC connection to the grid.

7. Solar PV System Design for an Urban Community

For the community-wide or district level solar PV system design, usually, the goal is to design a PV system that reduces the total energy demand in the community or even to reach zero-net in terms of electricity usage. Thus it is important to understand the solar PV installation potential and estimate the annual energy yield. This section describes the potential of solar energy production of Oak View Community in Huntington Beach based on community sectors and their functionality. The section also lists the steps and assumptions used to establish the sample model that is used in the analysis. Three scenarios are introduced

7.1 Introduction of the Oak View Community

The Oak View community is comprised of three major sectors, as seen in Figure 40: Commercial & Industrial (C&I), School Commercial, and Residential. Each of these sectors was further divided into several sections for the convenience of analysis. In order to produce a more convincing community energy and power analysis in the later sections. The hourly demand for the community is needed to conduct further analysis on net demand, and solar penetration. The demand for each community sector: C&I, School Commercial, and Residential are modeled by using the software OpenStudio. There are two outputs from OpenStudio, which are the electricity, and natural gas consumption profiles. For the purpose of solar analysis, only the electricity demand is used to generate meaningful results. The demand pattern for each sector has certain degrees of variation due to its unique functionality and operating schedules, which will be introduced in this section.

Figure 40. The aerial view of the Oak View community and its three major sectors: Commercial & Industrial (green), School Commercial (yellow), and Residential (red)

7.1.1 Commercial & Industrial Sector

The central section of the C&I corridor is referred to as the industrial portion of the C&I corridor. The two industrial customers in the C&I corridor are Republic Environmental Services and Zodiac Aerospace has shown in Figure 41. Together, they consist of nearly half of the available rooftop space in this sector including seven major industrial buildings and four major parking zones. At the north and south ends of the Commercial & Industrial (C&I) sector, there are commercial buildings henceforth referred to as the commercial portion of the C&I corridor as shown in Figure 42 and Figure 43. Further investigation of roof conditions and structural compatibility with PV technologies is necessary to confirm that these spaces are suitable for PV installation.

Figure 41. The industrial facility of the C&I Sector [40]

There are also large spaces in the north and south commercial areas include eleven major buildings and nine parking zones that are potentially suitable for solar PV installation.

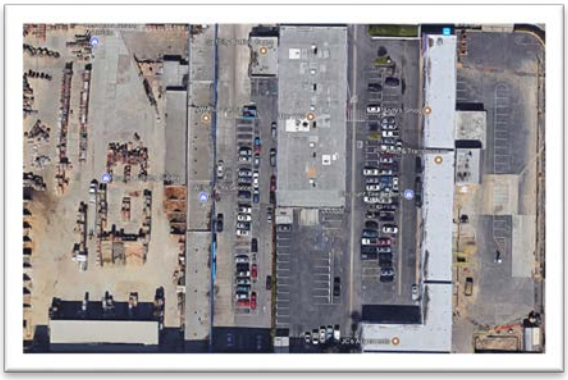

Figure 42. The north commercial area of the C&I Sector [40]

Figure 43. The south commercial area of the C&I Sector [40]

The plot shown in Figure 44 represents the aggregated electricity demand profile of a typical weekend and weekdays for the C&I sector of the community. It can be seen that the operation seems largely reduced from hour 78 to hour 92 on the weekend. The peak operation is typically around 2.5 MW during the workdays.

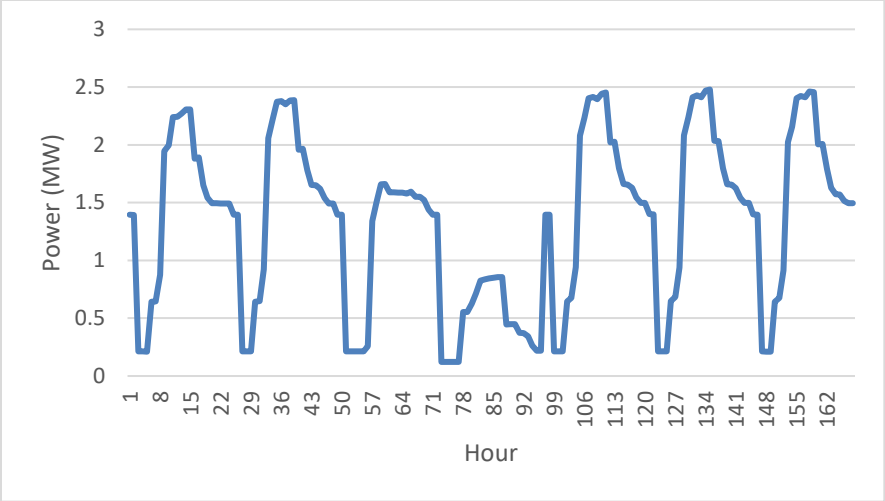

Figure 44. The C&I hourly demand for 7 continuous days from January 1st 24:00 to January 7th 23:00

7.1.2 School Commercial Sector

In the School Commercial sector, there are six major buildings: Oak View Preschool, Jeanne Hardy Head Start, Oak View Elementary School, Oak View Branch Library, Oak View Family Resource Center, and Oak View Child Care Center shown in Figure 45. This sector contains five major parking zones and twelve buildings as well as a future elementary school gym expansion.

Figure 45. The school commercial sector [40]

It can be seen from Figure 46 that the school commercial sector in the community operates on a relatively small load compare with the load of the C&I sector. On the weekends, the peak load is almost zero, which is a good representation of the load schedule of typical school operation.

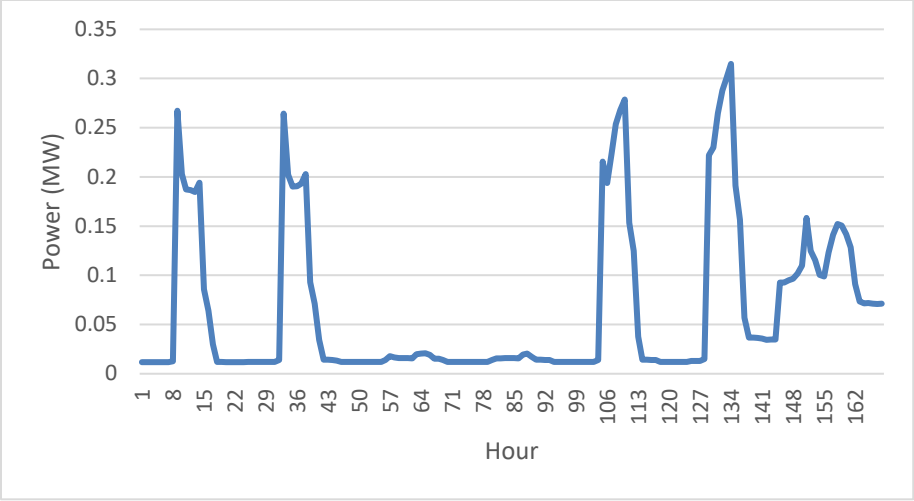

Figure 46. The school commercial hourly demand for 7 continuous days from January 1st 24:00 to January 7th 23:00

7.1.3 Residential Sector

The residential sector is the largest community sector by area and encompasses ten public parking areas and 266 individual buildings. This sector is divided into three sub-sectors: the South Residential (from Cypress Dr. to Sycamore Dr. and Fir Dr.) shown in Figure 47, the Central Residential (from Barton Dr. to Cypress Dr.) shown in Figure 48, and the North Residential (from Slater Ave. to Barton Dr.) shown in Figure 49.

Figure 47. The south residential sub-sector [40]

Figure 48. The central residential sub-sector [40]

Figure 49. The north residential sub-sector [40]

From
Figure 50, it can be seen that the output results of the aggregated residential sector include the morning and evening peak, and the evening peak is the highest during a day. The load profile for weekday and weekend looks identical.

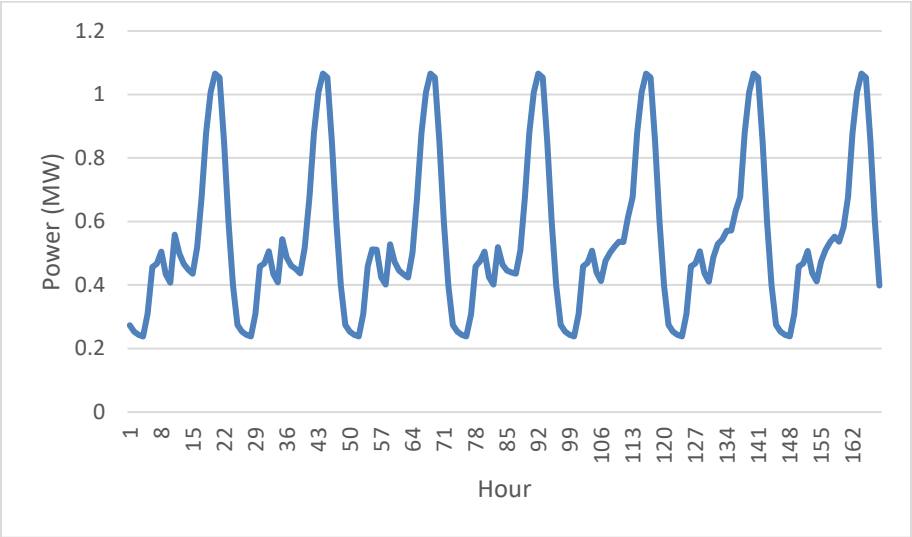

Figure 50. The residential hourly demand for 7 continuous days from January 1st 24:00 to January 7th 23:00

7.2 Commercial & Industrial Rooftop PV Design

The C&I sector in Oak View community involves only flat rooftop. Commercial and industrial rooftop usually has a large amount available roof area for solar PV installation, there will also be obstacles such as ventilation and HVAC units. For a flat roof, the fixed-tilt installation method is most viable. With the large area and free azimuth angle of the modules, facing south with relatively low tilting angle such as 5° would allow a high number of solar module installation and maximum energy production but with relatively lower kWh/kWp ratio. According to Cal Fire Department, if either axis of the building is 250 feet or less, there should be a minimum four feet wide clear perimeter around the edges of the roof. Otherwise, there should be a minimum six-foot-wide clear perimeter around the edges of the roof [38]. The centerline axis pathway should be provided in both axis of the roof, generally, the pathway should be a straight line not less than 4 feet and a 4 feet clearance around the skylight, ventilation, roof standpipes, and roof edges shown in Figure 51.

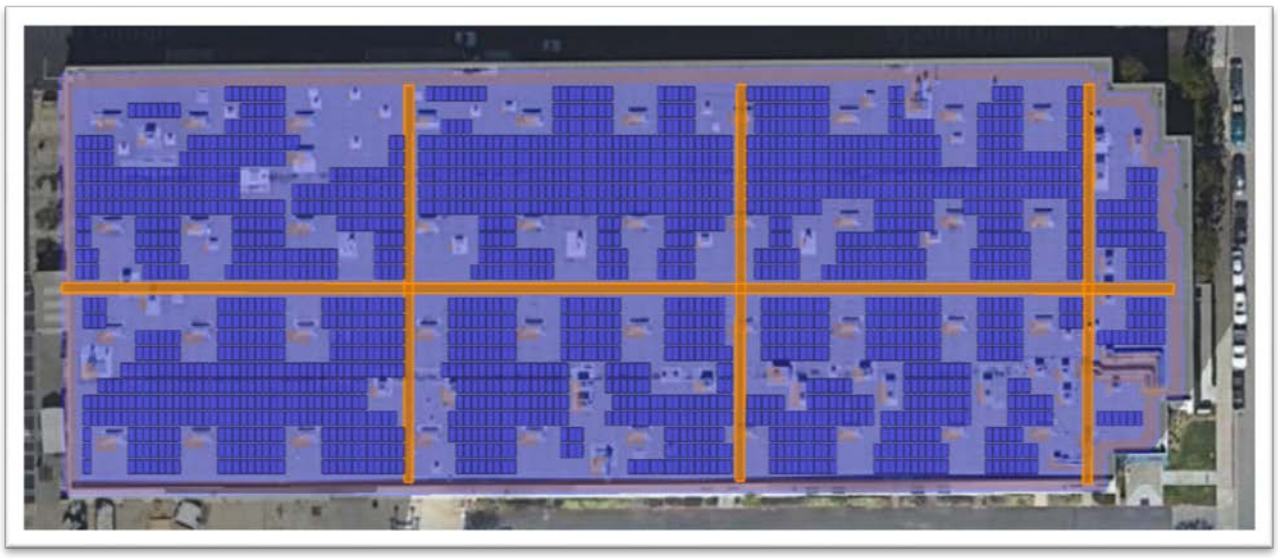

Figure 51. The commercial and industrial rooftop PV system design with rules and requirements applied

Besides the roof design guidelines from the fire department, the roof conditions in C&I sector needs to be determined by conducting survey or field trips. For example, the rooftop located at the Republic in Oak View is not designed to support PV arrays according to staff working at the Republic waste treatment facility and this could reduce a larger amount of PV installation potential.

7.3 Residential Rooftop PV Design

For residential PV system design in a community, the shading, obstacle, layout rules, and the energy yield are usually top factors for designers to consider. The tilted and flat roof pieces are the major target spaces to place solar modules with two different racking systems, the fixed tilted racking with constant tilting angle and the flush-mounted racking installation. Comparing the two types of racking of solar installation, according to the simulation from Helioscope, for the same number of solar modules facing 180 degrees with 15-degree tilt, the flat roof with fixed-tilt array has higher overall system efficiency primarily due to the low-temperature loss. From maximizing energy production perspective, for an area-constrained flat rooftop, it is not desired to tilt the solar array at its optimal tilt because in order to avoid self-shading less row can be installed if the module

tilting angle is large with respect to the surface. Therefore to maximize energy production and improve system efficiency it is desired to choose a flat roof in the community and keep the array with a relatively low tilt to fit more panels. The setback from roof edges should be 3 feet, any obstacle on the rooftop needs to be drawn out and shading impact to the nearby modules. For the tilted roof surface, there are mainly four types of roof structures in Oak View community: cross gable roof, cross gable with the valley, full gable, and full hip roof. For all of the four types of roofs, the modules should be no higher than three feet from the ridge and hip. For a roof with the hip layout, there should be at least one three-foot-wide clear access pathway from eave to the ridge on each roof slope where modules are located. For a single ridge rooftop, there should be two three-foot-wide access pathway from eave to the ridge on each roof slope where modules are located. Lastly, for the hips and valley type of rooftop, modules should be located no closer than one and one-half feet to a hip or a valley if modules are to be placed on both sides of a hip or valley. If modules are only located on one side of a hip or valley, then the modules can be placed directly abjectly to the hip or valley according to the Cali Fire Department [38]. While in the software Helioscope, once the setback is set, the setback length applies to all the edges of a roof segment that cannot be modified. Therefore, the number of PV panels created on each tilted roof surface will be a conservative value for this analysis.

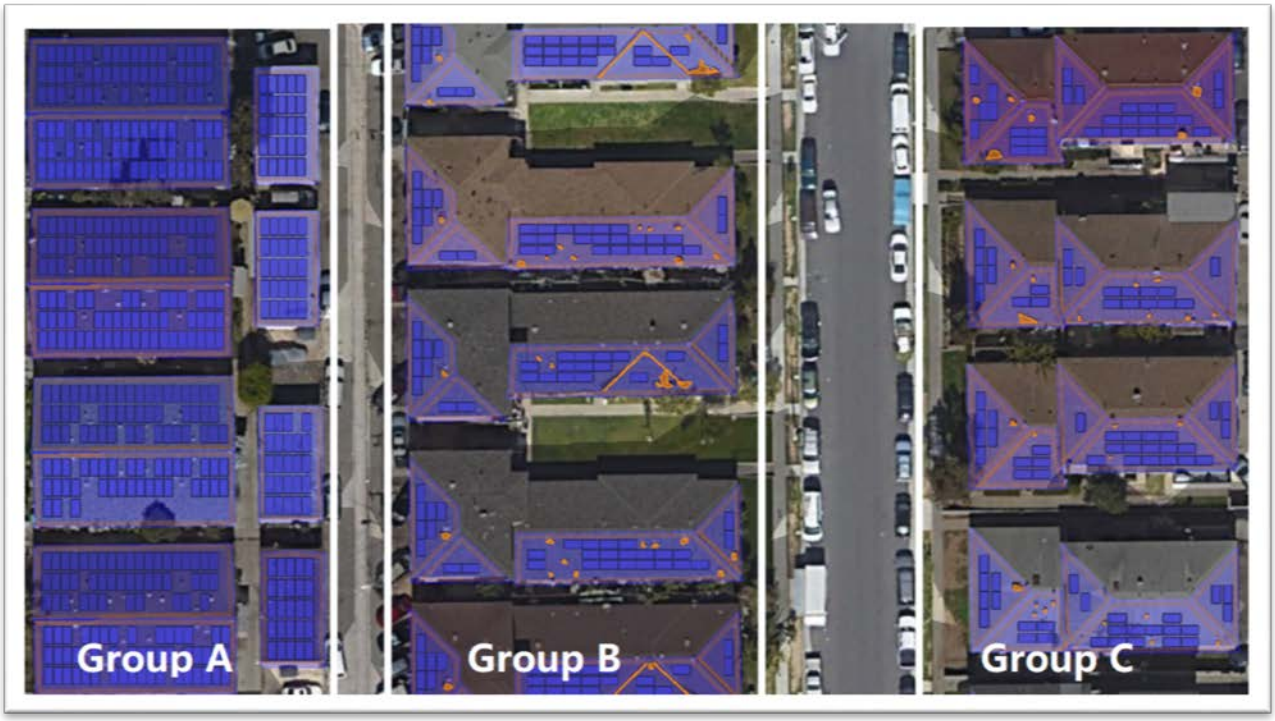

Figure 52. A community solar PV system design approach and consideration for different residential rooftop structures

In Figure 52, there are three groups of houses. Roofs in Group A contains a large amount of north and south-facing roof segments and the obstruction is concentrated at the ridge of the roof. Even though the north-facing roof has about 20% lower energy annual production than that of the south-facing surface if they are tilting at 14.04° from Helioscope analysis. The north-facing area could host a large amount of module installation, thus enable the possible installation on the north-facing surface. The garages located on the right side of the houses in Group A are placed with fixed tilted modules with 5° tilt. For group B the north-facing rooftop area are relatively smaller compared with that of Group A, if the setback is added, then the available area will be much less. Also, the east-facing roof segment contains multiple obstructions, those segments are the non-ideal location to place solar modules. Therefore, such type of rooftop is not recommended to utilize north-facing and east-facing roof segments. For Group C it is not desired to place solar modules on the north roof segments because of the low amount of irradiance. Not every rooftop in Group C contains the

same number of obstruction, therefore even for the same building type, module placement on each roof needs to be carefully analyzed. In addition, having solar modules placed on different oriented roof segments will create challenges for inverter sizing especially for small inverter without many MPP trackers.

7.4 Community Solar PV Zone-Map

For the PV system in the community, in order to establish the connection with the local power distribution system. The community is divided and recompiled into 41 zones based on the transformer location and the connection with nearby buildings shown in Figure 53. In each zone, there will be a limitation for the amount of PV to be installed due to the transformer capability. This method provides an easier pathway for a designer to further detail and investigate the distribution grid limitation in each community sector. One example of this method will be given below for one of the zones, AI, which is located in the middle bottom of the zone-map.

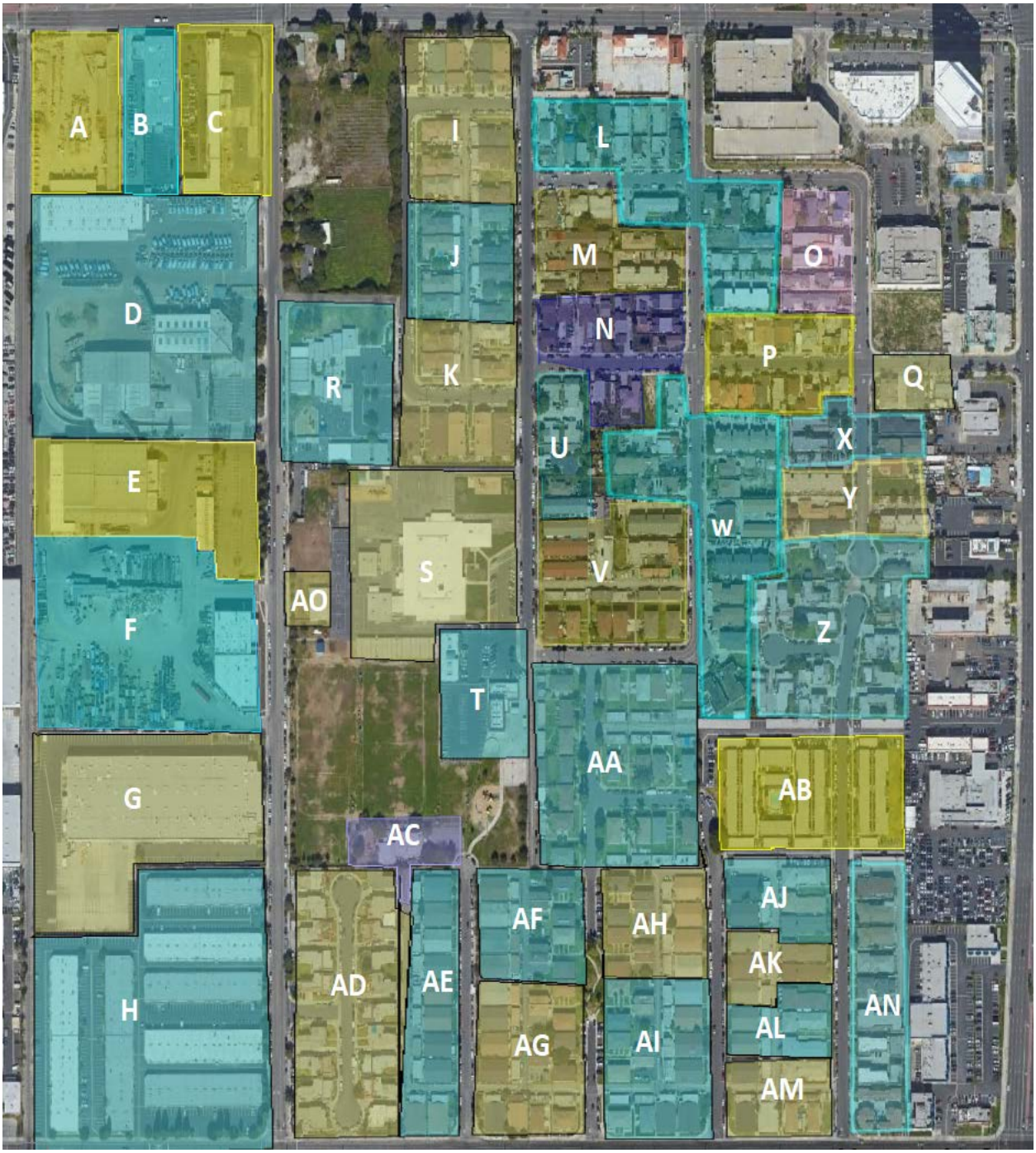

Figure 53. The solar PV zone-map created in Oak View community with 41 potential PV installation zones from A to AO

Figure 54. Zone AI with all the building structures labeled with numbers

Table 2. Sample documentation of five buildings at zone AI with address and array DC nameplate

Zone AI				
Community Sector	***Address***	**Label**	**# of Modules**	**DC Nameplate**
South Residential	17412 Koledo Ln	AI-1	8	2.64 kW
South Residential	17422 Kolden Ln	AI-3	11	3.63 kW
South Residential	17421 Queens Ln (Parking)	AI-8	25	8.25 kW
South Residential	17421 Queens Ln	AI-12	83	27.39 kW
South Residential	*7791 Slater Ave*	AI-20	23	7.59 kW
Total			**150**	**49.50 kW**

The building address and the corresponding PV capacity is documented for different scenarios and case studies. As shown in Table 2, a representative table listing the details of building and PV potential according could streamline the statistical process and provide convenience for future modification on the design.

7.5 Community Solar PV Design Scenarios

In this section, two design scenarios of community solar PV design are presented to estimate the installation and energy production potential. The first scenario is the maximum PV installation scenario in which the PV modules are installed at every possible location in the community as long as the space is available. The second scenario is based on the transformer location and the limitation of its size to prevent overloading.

7.5.1 Maximum Scenario

In the Maximum Scenario shown in a map overview in Figure 55, all of the roof and carport spaces are covered with solar modules with obstruction drawn out. The maximum solar PV potential is discovered, and no constraint is applied for such an optimistic scenario. Under this scenario, every possible location in the community such as car garage, open parking space, and playground are considered to place solar PV modules to demonstrate the maximum capacity of solar PV could be deployed in the community. The PV installation potential and energy production from each sector are shown in Table 3. Meanwhile, Figure 56 and Figure 57 are made to better visually represent the size of PV deployment in each community sector.

Figure 55. Oak View Community solar PV system design overview under the Maximum Scenario

Table 3. Solar PV potential and energy production broken down for all community sectors under Maximum Scenario

Oak View Community (Maximum Scenario)	C&I Sector	School Sector	Residential Sector	Community Total
PV Capacity (MW)	7.42	1.38	6.06	14.86
Annual Production (GWh)	11.31	2.03	8.71	22.05
kWh/kWp	1,513	1,476	1,436	1,477
System Performance (%)	80.3%	80.4%	77.0%	79%

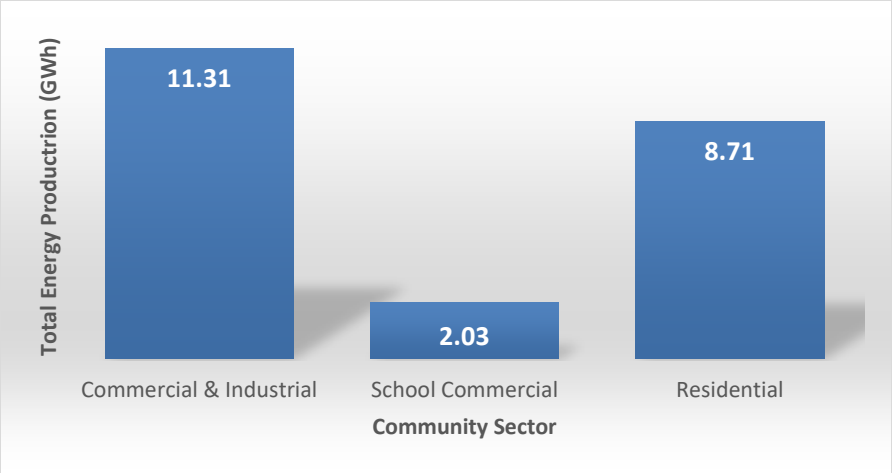

Figure 56. The annual solar production based on each community sector under Maximum Scenario

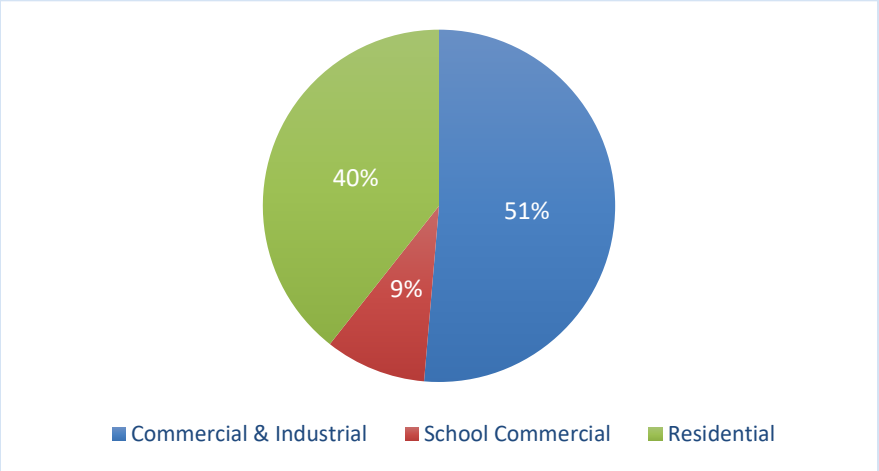

Figure 57. The annual solar production from the C&I, school commercial, and residential by percentage under Maximum Scenario

7.5.1.1 C&I Sector under Maximum Scenario

Under the Maximum Scenario, the Commercial & Industrial sector could potentially install 7.42 MW of solar PV. The breakdown by entities in the sector is shown in Figure 58, and types of the PV installation is shown in Figure 59.

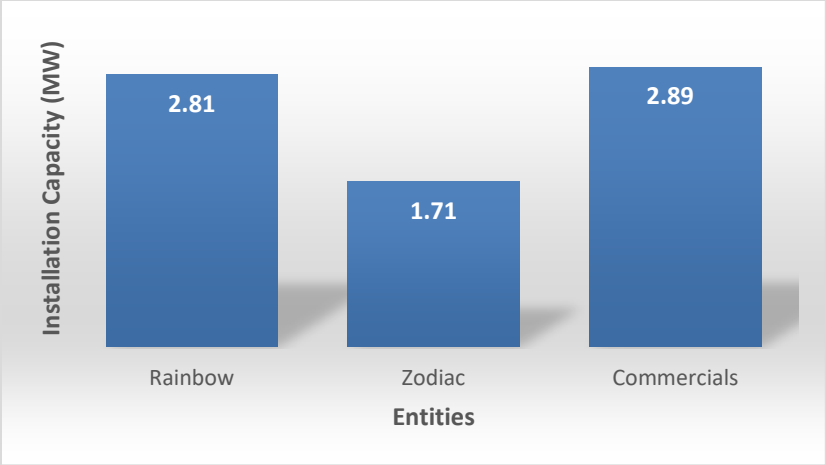

Figure 58. The C&I sector installation capacity based on local entity under Maximum Scenario

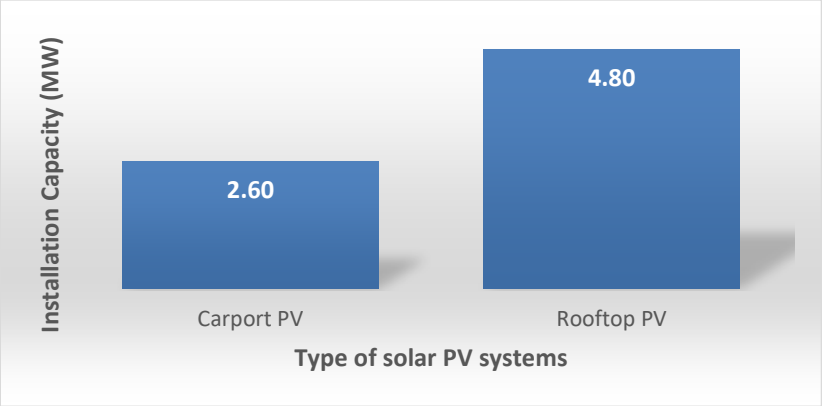

Figure 59. The C&I sector installation capacity based on the type of PV system under Maximum Scenario

7.5.1.2 School Commercial Sector under Maximum Scenario

Under the Maximum Scenario, the School Commercial sector could potentially install 1.38 MW of solar PV. The breakdown by entities in the sector is shown in Figure 60, and types of the PV installation is shown in Figure 61.

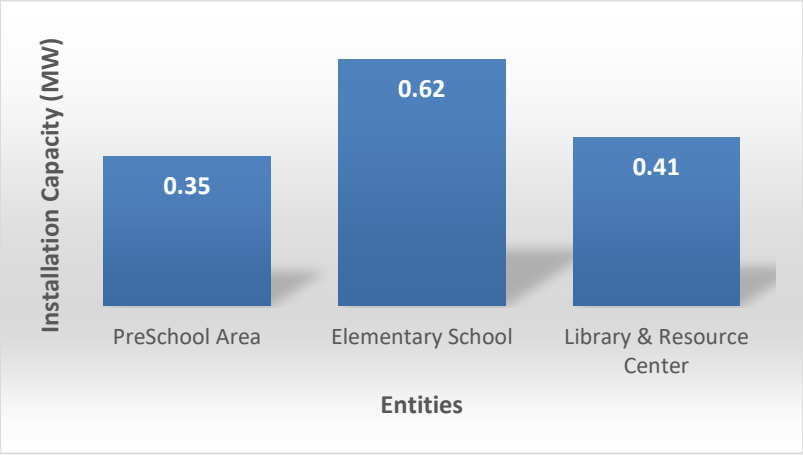

Figure 60. The school commercial sector installation capacity based on local entity under Maximum Scenario

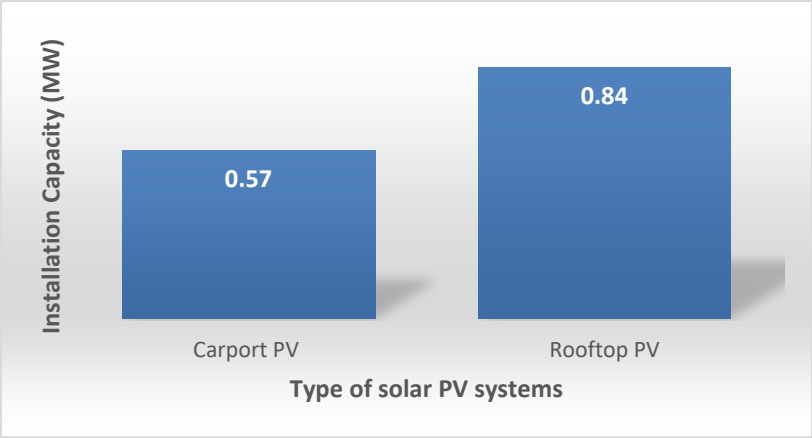

Figure 61. The school commercial sector installation capacity based on the type of PV systems under Maximum Scenario

7.5.1.3 Residential Sector under Maximum Scenario

Under the Maximum Scenario, the Residential sector could potentially install 6.06 MW of solar PV. The breakdown by streets in the sector is shown in Figure 62.

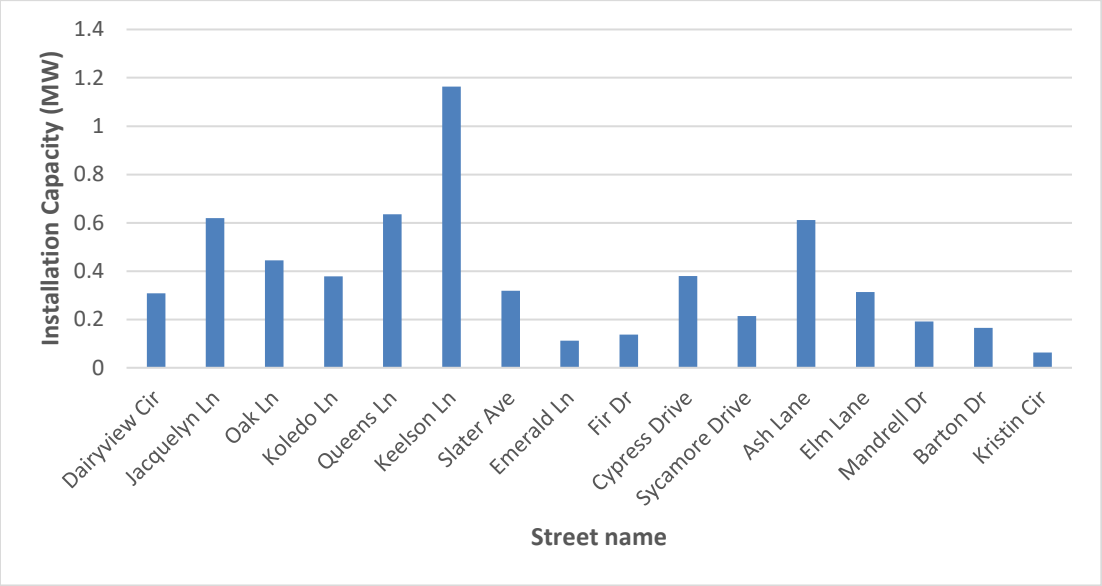

Figure 62. The solar PV installation capacity by streets in the entire residential sector under Maximum Scenario

7.5.2 Realistic Scenario

In the realistic scenario with a map overview shown in Figure 63, each PV zone in the community is given a limitation of the amount of PV that can be deployed in that specific sector is shown in Table 4. The installation breakdown is shown in Figure 64 and Figure 65. The determination is made based on the transformer rating such as power and voltage as well as the corresponding power flow. Those factors become the constraint for how much PV each zone could potentially deploy without causing damage to the local power distribution system. Therefore, the PV installation potential has been dramatically reduced in the community. The total PV potential in a realistic scenario is reduced by almost 57% of the maximum scenario. Therefore, the actual size

of the community PV installation also depends on the capacity and limitation of the local electrical infrastructure.

Figure 63. Oak View Community solar PV system overview under the Realistic Scenario

Table 4. Solar PV potential and energy production broken down for all community sectors under Realistic Scenario

Oak View Community (Realistic Scenario)	C&I Sector	School Sector	Residential Sector	Community Total
PV Capacity (MW)	3.62	0.66	1.73	6.01
Annual Production (GWh)	5.50	0.97	2.65	9.12
kWh/kWp	1,521	1,463	1,525	1,515
System Performance (%)	79.5%	79.3%	78.4%	79.2%

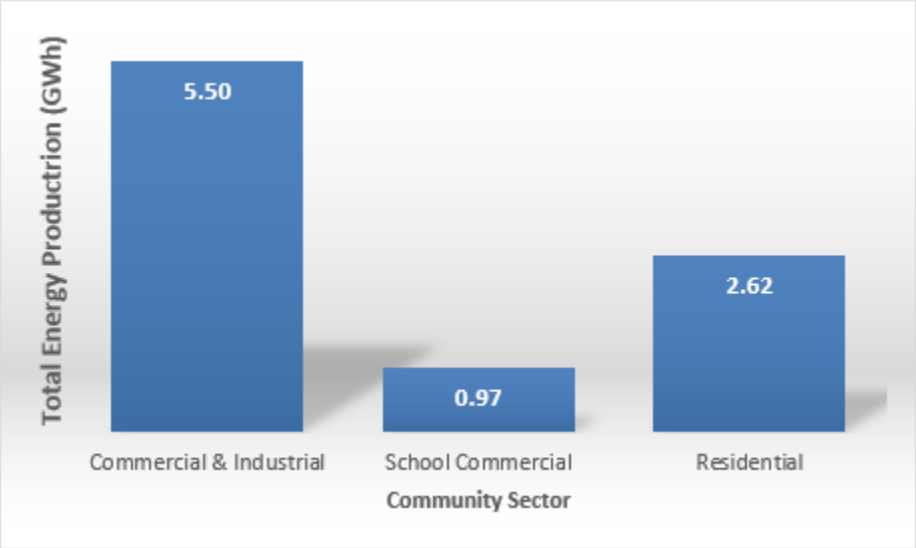

Figure 64. The annual solar production based on each community sector under Realistic Scenario

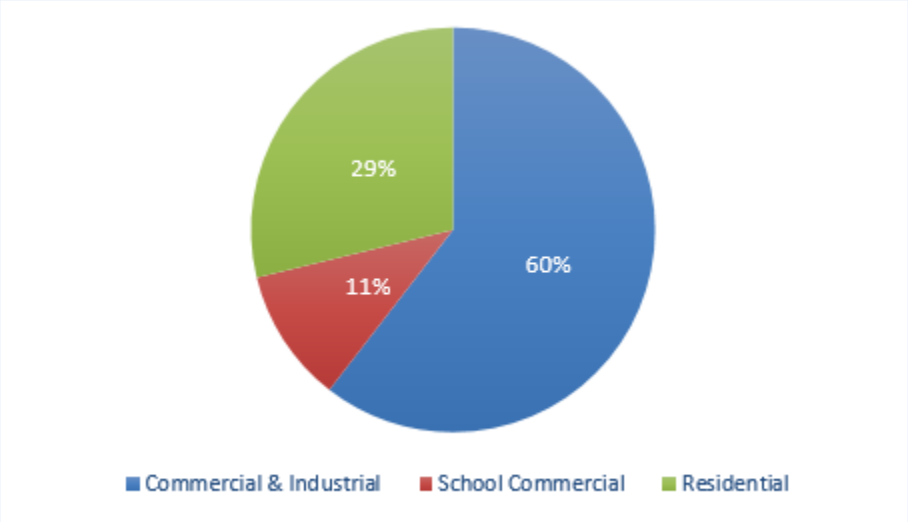

Figure 65. The annual solar production from the C&I, school commercial, and residential by percentage under Realistic Scenario

7.5.2.1 C&I Sector under Realistic Scenario

Under the Realistic Scenario, the Commercial & Industrial sector can install 3.62 MW of solar PV. The breakdown by entities in the sector is shown in Figure 66, and types of the PV installation is shown in Figure 67.

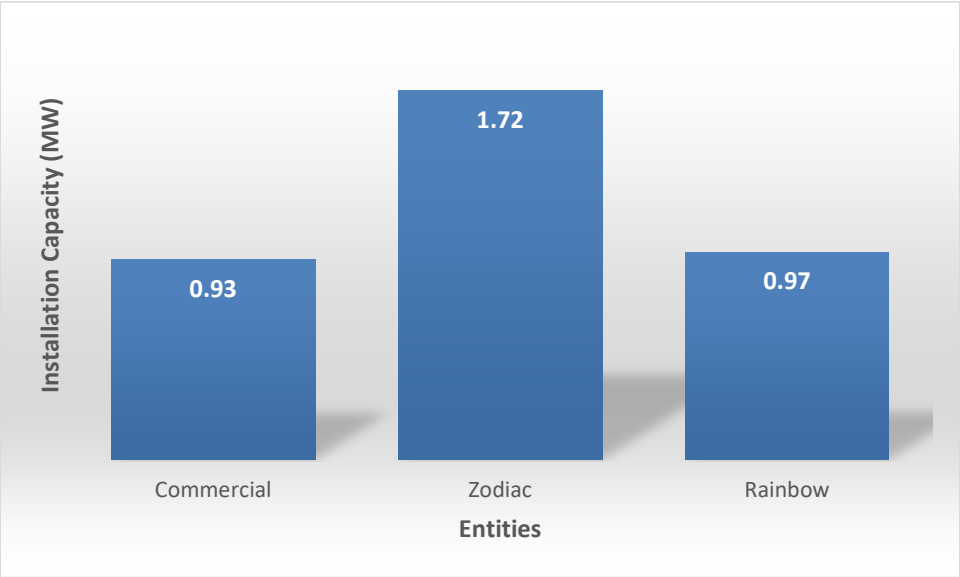

Figure 66. The C&I sector installation capacity based on local entity under Realistic Scenario

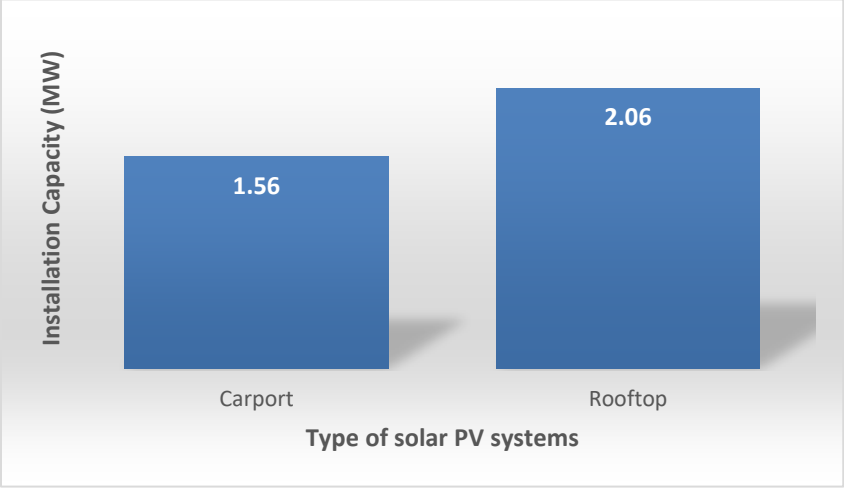

Figure 67. The C&I sector installation capacity based on the type of PV systems under Realistic Scenario

7.5.2.2 School Commercial Sector under Realistic Scenario

Under the Realistic Scenario, the School Commercial sector could potentially install 0.66 MW of solar PV. The breakdown by entities in the sector is shown in Figure 68, and types of the PV installation is shown in Figure 69.

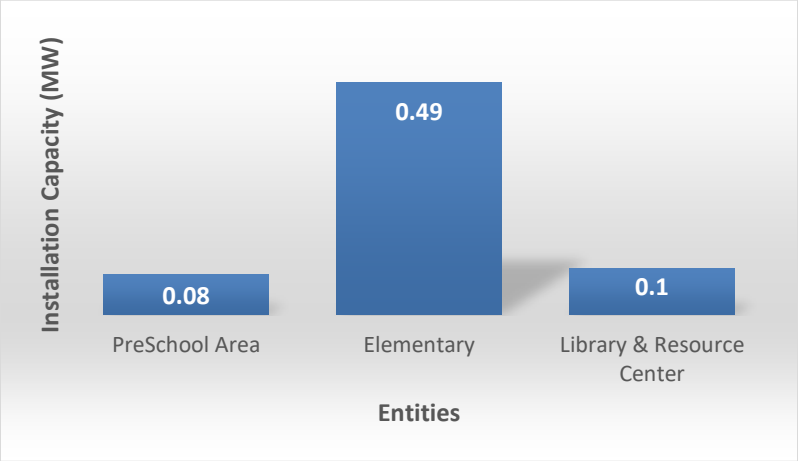

Figure 68. The school commercial sector installation capacity based on local entity under Realistic Scenario

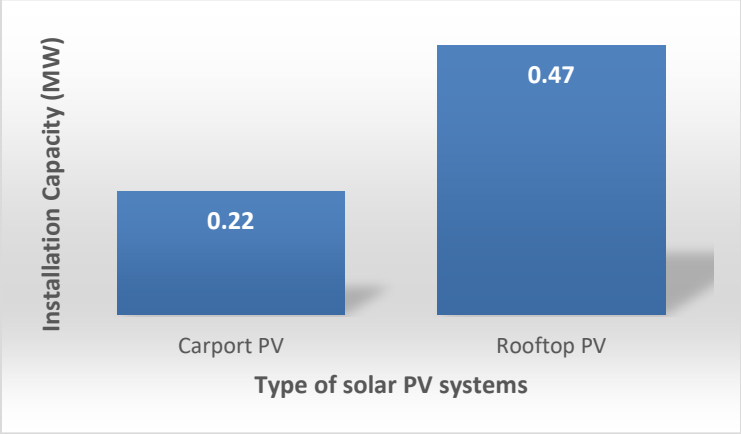

Figure 69. The school commercial sector installation capacity based on the type of PV systems under Realistic Scenario

7.5.2.3 Residential Sector under Realistic Scenario

Under the Realistic Scenario, the Residential sector could potentially install 1.73 MW of solar PV. The breakdown by streets in the sector is shown in Figure 70.

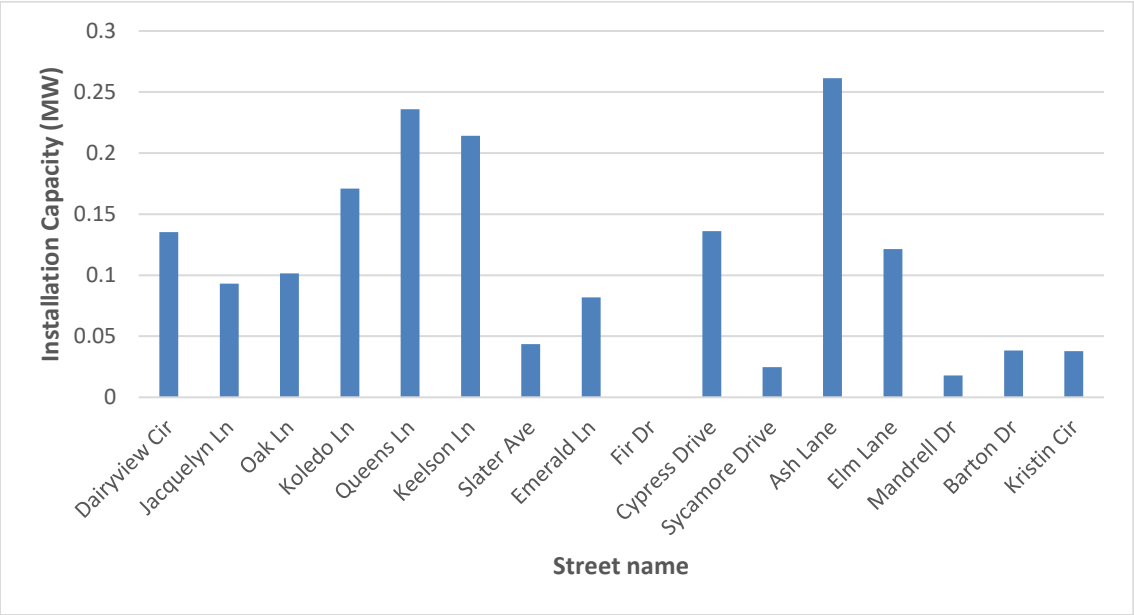

Figure 70. The solar PV installation capacity by streets in the entire residential sector under Realistic Scenario

7.6 Analysis of Community Solar PV Energy Yield

For the Oak View community, the results of the maximum scenario are used to demonstrate analyses on the solar energy yield of the community. The annual, seasonal, and monthly production of solar energy in the Oak View community is analyzed. In addition, the energy production from each community sector and even the streets are presented in this section. The detailed PV installation capacity in the community is recorded in a detailed fashion which could provide significant benefits for modification on the design at any later time. From a project administrative prospective, the data analysis and statistical representation are crucial when present the analyzed results of a community solar project.

7.6.1 Annual & Seasonal Solar PV Production

In this subsection, the solar energy production through a calendar year is presented in four seasons as March, June, September, and December. Since the resolution of TMY3 weather data is with the hourly interval, thus the results are analyzed in either daily or hourly fashion to demonstrate the

unique features of seasonal variability of the solar energy yield. In addition, the maximum and minimum energy production days from an entire year are also shown. The energy yield from each sector is calculated and presented here. Figure 56 and Figure 57 show the community's annual energy production in all three sectors, the commercial and industrial contributes the most and followed by the residential sector.

The curves in Figure 71 represents the daily production for March, June, September, and December. This gives a general sense of how the solar daily production varies within each season. As shown in Figure 71, the production trend of June is increasing from the beginning to the end of the month, which is the month that has the highest solar production. The general production trends of September and December are decreasing.

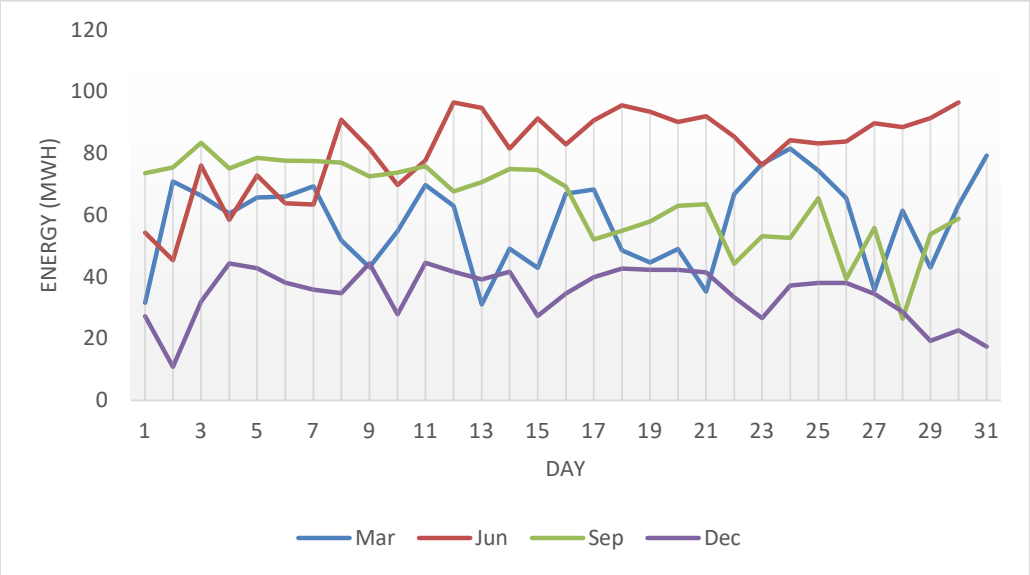

Figure 71. Seasonal solar production with daily variation for four chosen months under Maximum Scenario

Figure 72 presents the hourly average value of solar production for March, June, September, and December to display differences for the same hour during the day. Usually, the largest variation

occurs in the evening. In the morning, the difference and variation are smaller between winter and summer. This plot could provide some insight into seasonal energy storage and dispatch strategy.

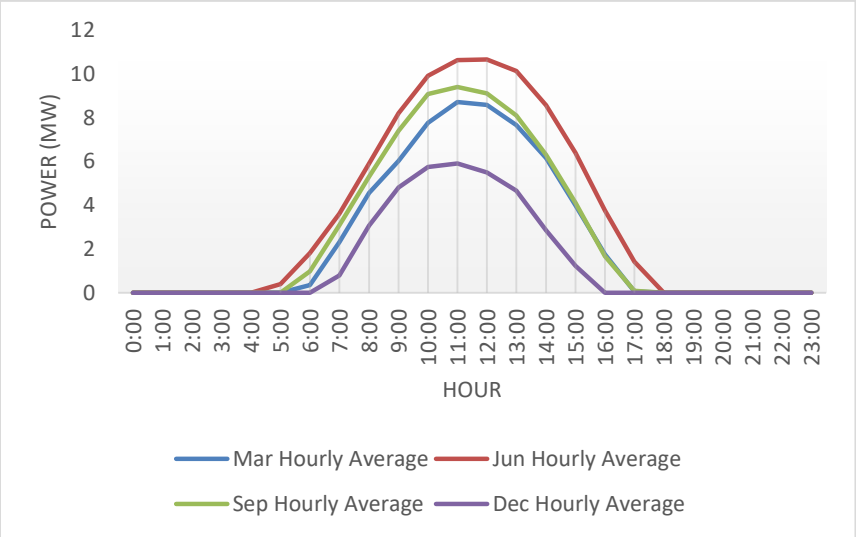

Figure 72. The hourly average seasonal solar production curve for the four chosen months under Maximum Scenario

It is interesting to observe the maximum day and minimum day solar production and compare it with the difference between the two on the hourly scale within one chart shown in Figure 73. This gives a general sense of how much solar production could vary within a year, from its maximum day to minimum day. It can also be seen the effective hours of the solar production period during the 24 hour period. For the minimum day in winter on December 02, the solar production starts around 7 AM (non-local time) and ends around 4 PM. In contrast, for the maximum day, solar production roughly starts at 4 to 5 AM and ends at 6 PM. The difference in the morning is roughly 3 hours in winter compared with the time in summer.

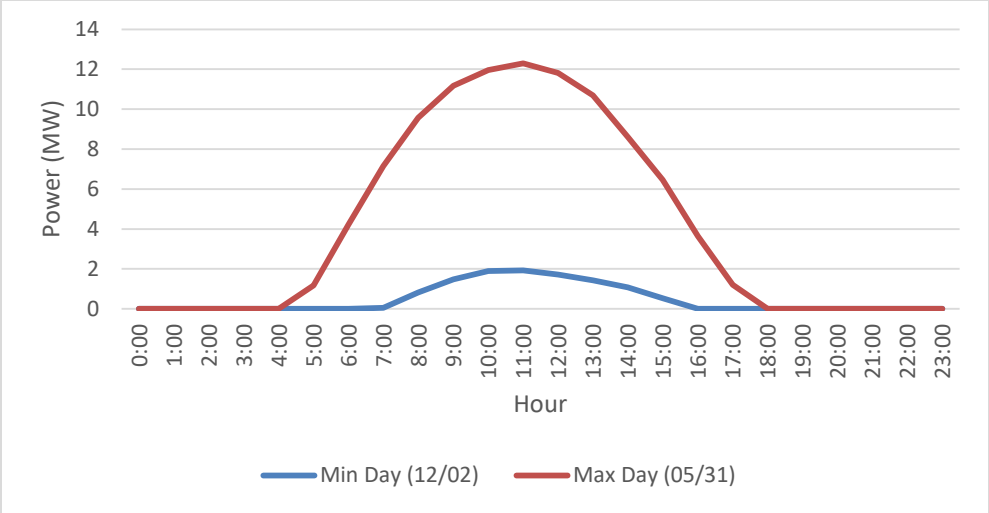

Figure 73. The maximum and minimum solar production day of the calendar year under Maximum Scenario

For the maximum day for both scenarios, the peak power is reduced from 12.30 MW and the minimum day peak is at 1.93 MW.

By plotting daily solar production over a year span, it is easily seen how the daily solar production could vary between two adjacent days within a calendar year shown in Figure 74. The red line is an average value of daily solar production throughout the year. It suggests most days in the summer are above the average line, with occasional exception due to weather variation.

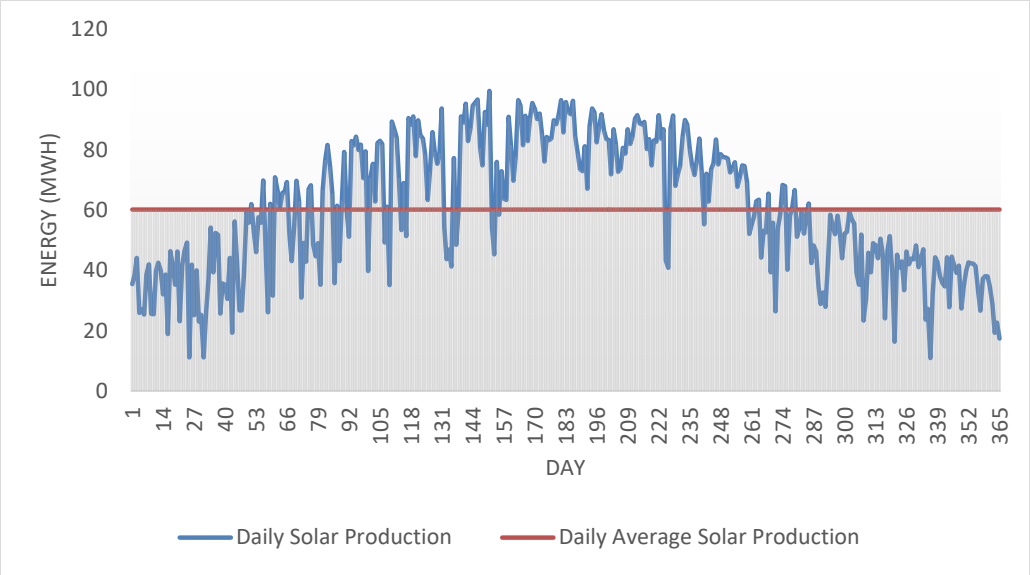

Figure 74. Day to day solar production variations during a calendar year under Maximum Scenario

For a solar PV project, the most important plot to visualize system yield would be the monthly energy yield chart. By plot each month's total solar production in Figure 75, one could easily notice the production for each month and make an educated decision on system and the row distance sizing to maximize the total system performance. For instance, if the energy production in the winter months is several-fold lower than that of the summer months, the designer may not use the effective hours of the winter solstice to determine the row distance instead of focusing on the effective hours on the summer or springtime to size the system.

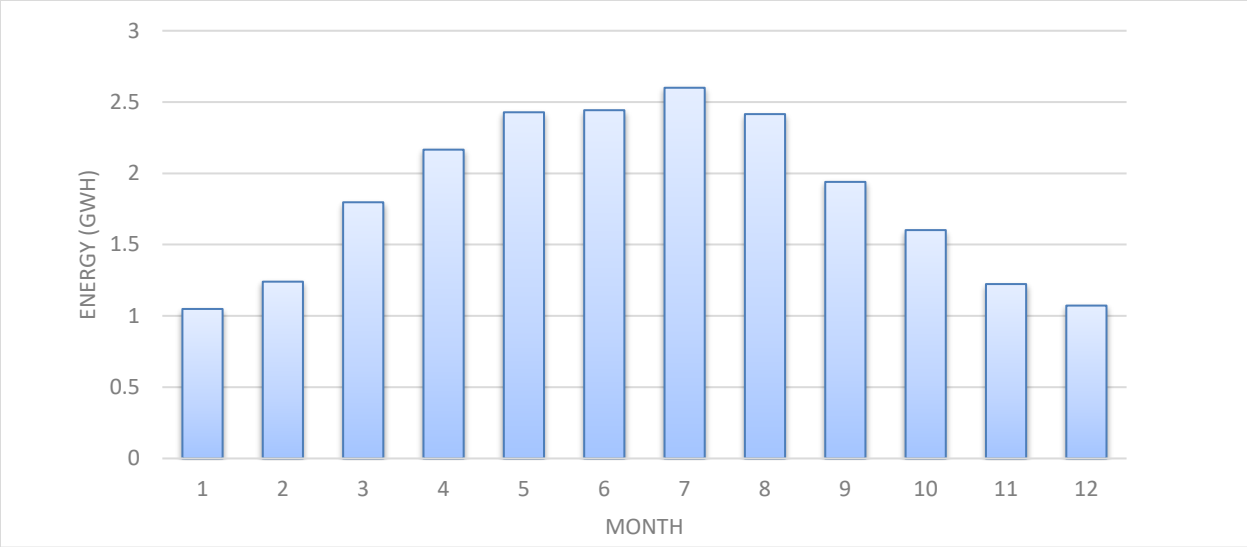

Figure 75. Monthly solar production under Maximum Scenario

7.6.2 Hourly Average Solar PV Production

For the chosen four months that represent the seasonal solar production variation. It is noticed that the summer month June represents the best performance among other season months. For the demonstration purposes, the sample month is chosen to be June in this section, one of the summer months, which has relatively high solar energy production. The hourly average value for each hour of the month of June is calculated. In order to investigate the net-load curve of June, the load data obtained from OpenStudio is also processed in the same fashion as the hourly average for each hour. Besides the average of each hour, the first and second standard deviation value of the solar energy data of the community under maximum scenario is also calculated to better understand the variation of the solar production at each hour of a 24 hour period.

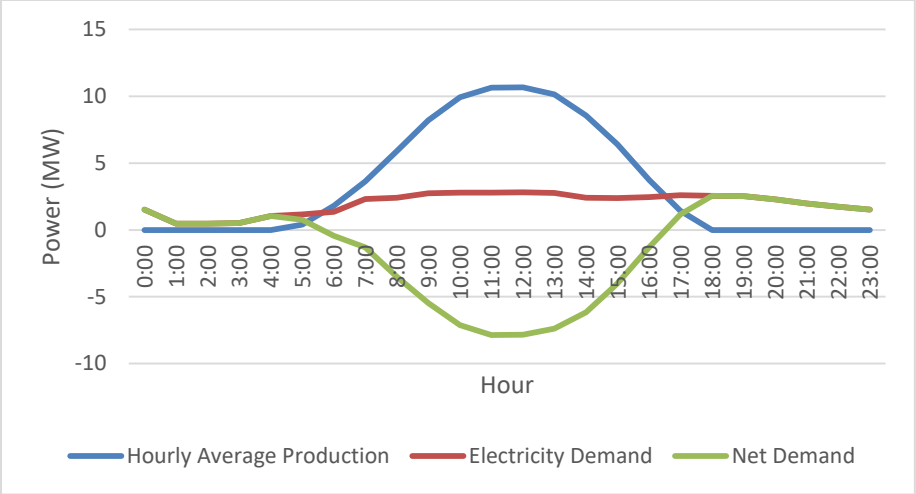

Figure 76. Hourly average demand, production, and the net demand of June under Maximum Scenario

From Figure 76, the electricity demand of the community is the highest during the day which is mainly due to the activity at the C&I and the school sector. The solar production is also high at the noon but is much greater than the demand thus results in a negative net-load or surplus solar energy in the community during the day. In the evening, the demand is mainly due to the residential and C&I sector. The excess energy generated by solar PV during the day can either be curtailed directly or stored in the community to be used in the evening.

After introducing the hourly average solar production for the month of June, there is also a typical need for the designer to analyze the variation of solar production at each hour. Such an analysis would allow the designer to quickly realize the intermittency of solar production at each hour. Here, by applying and defining the lower and upper limits or bounds of the first standard deviation, 68.3% of the data would fall within the bounds as shown in Figure 77.

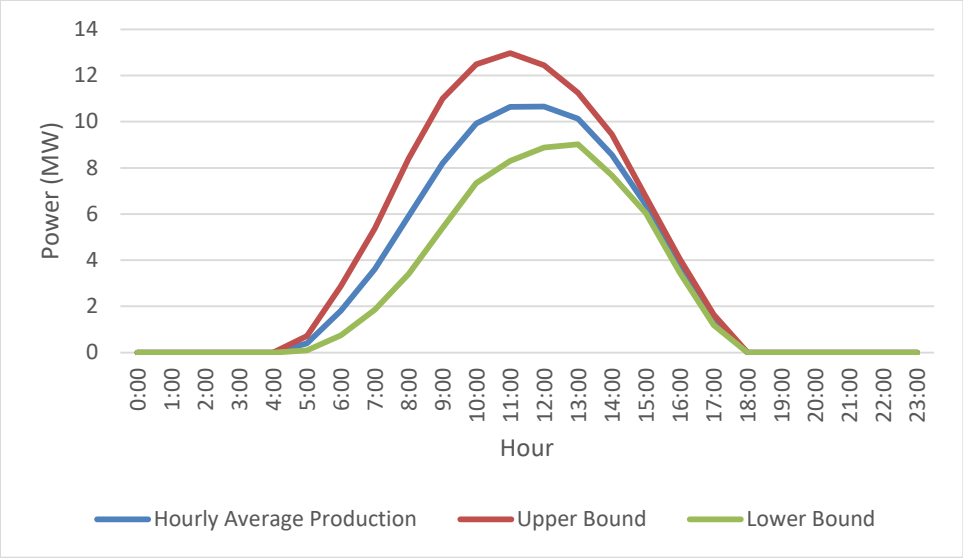

Figure 77. The hourly solar production profiles with one standard deviation bounds of June under Maximum Scenario

For the second standard deviation, 95.5% of the data will fall under these two bounds as shown in Figure 78.

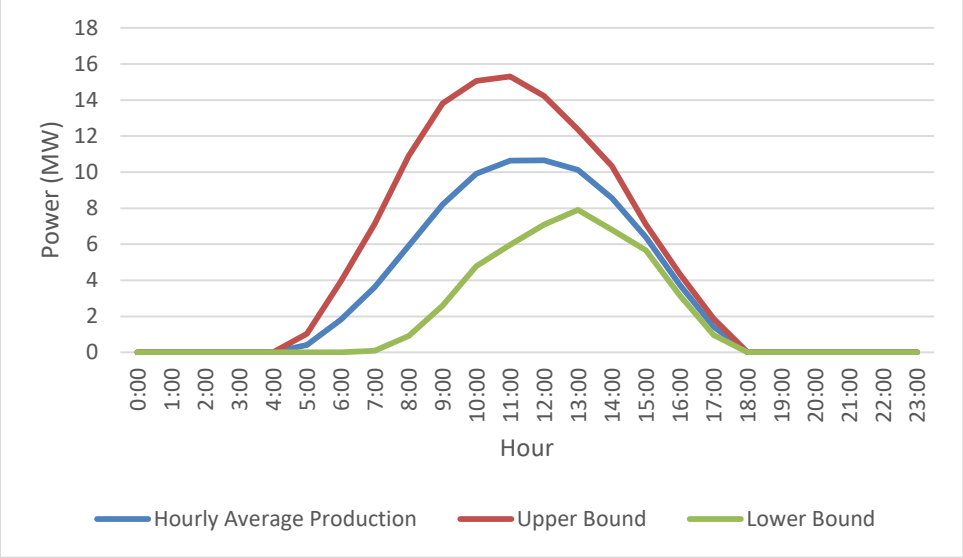

Figure 78. The hourly solar production profiles with two standard deviation bounds of June under Maximum Scenario

From Figure 77 and Figure 78, it can be easily observed that the largest hourly variation of solar production period is concentrated during the day from 4:00 AM to 1:00 PM, due to the marine

layer weather effect in the coastal region in summer months. In the afternoon and evening hours, the variation of solar production is very small.

For the community, the hourly average demand and solar production in June of each sector can be plotted together to compare the net-load contribution to the overall community energy surplus. In addition, the demand profile from each sector can also be clearly presented in the plot. In Figure 79, the load peak of the C&I sector is the highest and most concentrated during the day from 7 AM to 4 PM. The residential load includes the morning peak and an evening peak. The load profile of the school sector is the lowest. Therefore, the general strategy to most effectively offset the load for the community is to deploy large capacity at C&I sector, and facing south to offset the day peak during noon; deploy moderate amount of PV facing north-west direction in the residential sector to offset the evening peak; deploy the small amount of PV module facing north-east direction to offset the demand peak in the early morning and noon.

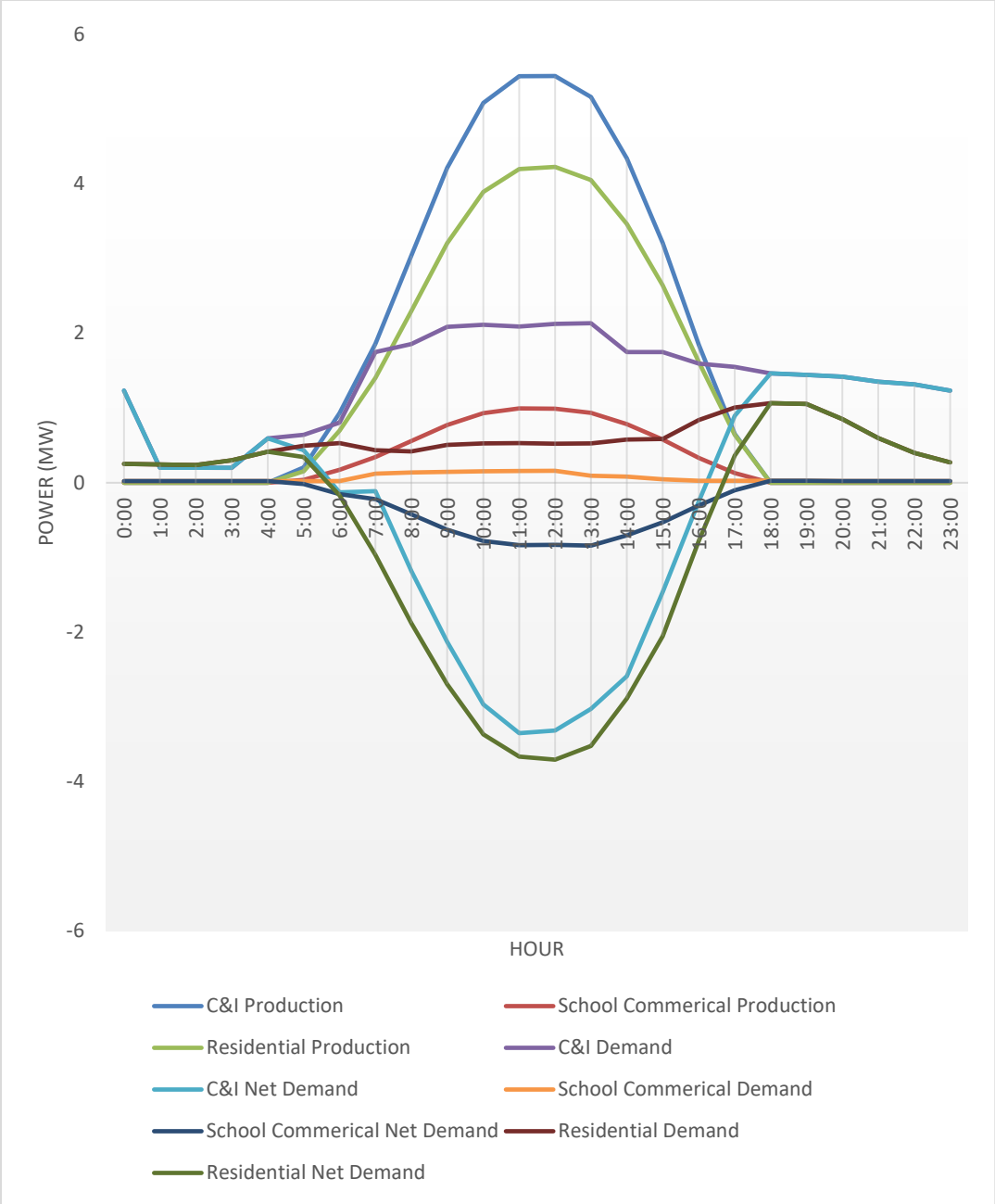

Figure 79. Demand, production, and net demand of each of the three community sectors under Maximum Scenario

7.6.3 Weather Influence on the Net Demand

The weather condition is the largest variable that determines the solar production profile. With a given load curve, the net-load then is generated based on the solar profile. For the coastal region of California, the typical marine layer effect is the most weather phenomena in the summer months.

From early morning to noon, due to the presents of the marine layer. The most amount irradiance from the sun is the sky-diffuse irradiance, since such layer block majority direct irradiance, the solar production is typically low in the morning as shown in Figure 80. At the noon around 12:00 PM to 1 PM, solar production suddenly increased due to the disappearance of the marine layer thus causing a peak. These types of analyses are important in case of unique weather status. A solar designer needs to ensure the electrical system and the supporting infrastructure could still operate normally under various local weather conditions. Since the overall demand of the community appears to be relatively flat dominated by the operations at the C&I sector, the net-load profile has a similar shape of the solar profile, thus the peak of the surplus energy of the day on June 1st also peaks at noon.

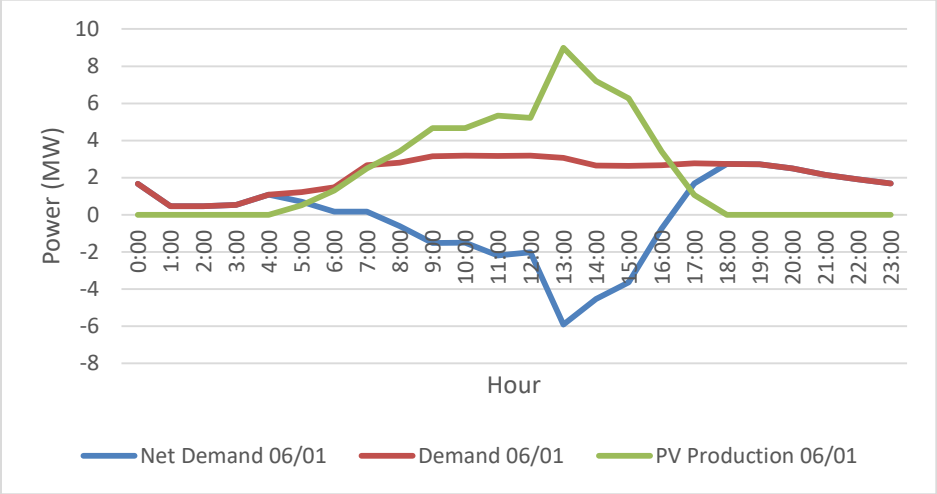

Figure 80. The influence of coastal weather on morning solar production on June 1st under Maximum Scenario

In Figure 81, on June 5th the solar production profile is suddenly flat from 10 AM to 11 AM and followed by a sudden drop from 11 AM to 12 PM. The possible explanation of such phenomena could be the effect of moving cloud in this region in the noontime. From 12 PM to 1 PM, immediately after the cloud leaves the community, the solar production peaks again. Comparing with the solar production profile of June 1st and that of June 5th, it is seen that the marine layer

effect in the coastal region has a bigger impact compare with cloudy weather effects in terms of the daily energy production unless the cloud would not move and last for a day. Thus, during the coastal weather condition, the demand response strategy needs to be further determined in order to better tackle the sudden peak due to the marine layer or the moving cloud.

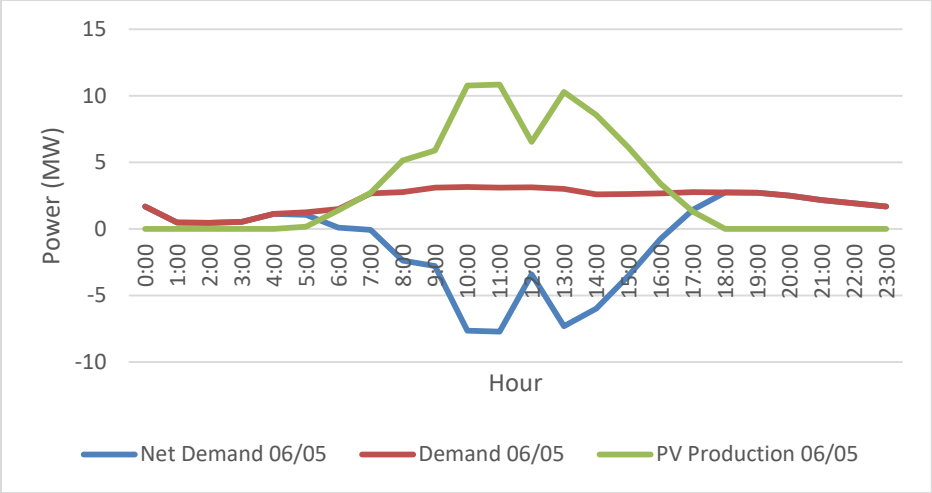

Figure 81. The influence of moving cloud on solar production on June 5th under Maximum Scenario

8. Summary & Conclusions

The installation of solar PV array on area-constrained rooftop surfaces especially in an urban context is investigated. For a constant tilted rooftop array, the irradiance received by the array is directly related to the shading and the number of rows of the module can be fit on the surface. In addition, a novel layout of the solar module, the incremental tilted layout, is presented in this work. The irradiance, DC energy yield, and panel economics are all analyzed and compared with those of the constant tilted array at various roof pitches and row distances. The procedure of designing a rooftop solar PV system using satellite image-based commercial software is also introduced in this work. Lastly, with the goal of increasing urban community renewable energy penetration, a sample community at Oak View, Huntington Beach is presented. A systematic approach to designing a community-wide solar PV system is introduced with a detailed analysis of the electricity demand, solar production, and net-load profile of the community.

8.1 Constant Tilted Rooftop Array with Area-Constrained

Results haven show that when maximizing irradiance received on an area-constrained surface, the local optimal tilting angle yields suboptimal results due to a) self-shading, or b) reducing the number of rows of panels to allow for sufficient row spacing to avoid self-shading. To maximize the irradiance received in a PV system on a defined surface, panels should occupy as much the rooftop area as possible first (i.e. laying the array flat). After the maximum number of rows has been added, the rows should be spaced such that the maximum tilt angle can be achieved such that no shading occurs.

Note that for small tilting angles (1-3° respect to the surface), there is minimal difference in energy production (<1% variation). In this instance, flush mounting is likely to nearly achieve the goal of maximizing irradiation absorption while avoiding the excess cost to create a small tilt. This, of

course, is not true as the tilting angle increase. For residential PV, the most convenient and economic installation solution is using flush-mounted racking for modules. Note, however, flush installation of PV on a flat surface reduces opportunities for self-cleaning. Higher tilt values allow gravity to keep panels clear of dust, dirt, and debris, especially when it rains. Soiling was not taken into account in the current work.

Other interpretations can be drawn from the previous simulations. Orientations besides the south should be also taken into account when installing panels, especially at lows latitudes and for small pitched roofs. Panels installed on the north, east and west sides of the roofs cannot be ignored since those roofs can potentially receive 80% of the irradiance compare to roofs that orientated south. Ultimately, the decision to install north-facing panels would be a tradeoff between the values of renewable generation or net-zero energy versus the higher cost of electricity.

8.2 Incremental Tilted Rooftop Array with Area-Constrained

From the analysis, it is found that the incremental tilted layout could potentially achieve better panel economics only at lower-pitched rooftop even under partial shading compare with constant tilt or flush-mounted layout on an area-constrained surface. When the incremental tilted array is placed on the low pitched (such as 5°) rooftops, if the DRPR is set at low range (such as 0% to 20%), it is desirable to tilt the array higher (such as a higher initial tilting angle of the most front row but with a low incremental tilting value such as 1°) towards local optimal to better harvest energy yield and improve panel economics; under severe shading situation (such as 50% PRDR), while managing more rows to be fitted on the rooftop, it is important to keep the array tilting angle to below in order to maximize energy yield, but will likely result with a poor panel economics comparing with the low PRDR scenario. Also, the low incremental tilting value (such as 1°) appears to be able to achieve better array energy production and better panel economics than high

incremental tilting values. It is also found that at various values of PRDR, the constant tilted array can always achieve better annual energy production than any of the incremental tilted array under partial shading conditions. For a certain degree pitched surface, it is found that at various PRDR, the annual irradiance received by an array (incremental or constant tilted) could remain relatively constant, but the energy production from the array starts to decrease as DRPR increases. Among south-facing roof with pitches ranging from 0° to 30° under various DRPR, it is found the PV arrays on medium roof pitches such as 15° and 20° could achieve the best energy production and panel economics for both incremental tilted array and the constant tilted array at the location of southern California. For an area-constrained rooftop surface, the energy production and panel economics not only depends on the partial shading but also the number of rows that can be installed on the rooftop. It is found for a pitched roof surface, the larger number of rows could lead to better irradiance received and better production relatively but poor panel economics especially under partial shading condition.

8.3 Community Solar PV Design

For a large multi-functional community with hundreds of buildings inbound, with the goal of increasing renewable energy penetration from local solar PV sources, the utilization of commercial software is essential to better design and plan the solar PV system with proper steps and procedures. In order to quickly estimate the solar installation potential with a limited site visit, it is recommended to use commercial solar design software with a satellite image, to begin with, the design process. The steps of successfully design community-wide solar PV project are to first understand the load profile and schedule from the different community sector, to identify the critical electrical infrastructure such as transformer, and to establish an efficient method of documentation such as a zone-map which is created in this work, to better organize the solar design.

For commercial and residential buildings, the design regulation and requirement from local authorities must be applied before any major design work is done. According to the reality of each community, several design scenarios need to be considered and proposed. Besides the two scenarios mentioned in this work, a certain specific scenario such as budget constraint is very likely to be presented in a community solar project. After careful design and planning of the PV system, it is important to analyze the energy production potential and draw the connection with the current existing electricity demand. The analysis done in this work including the study of intermittency of local solar energy production and the variation of production from day to day and hour to hour because such analysis could provide insights on decision-making process of sizing energy storage system and the understanding of potential impact of local electrical infrastructures such as power flow and overloading of transformer. It is found in this work that in the month of June, the marine layer effect could have the largest solar generation reduction of a day compared with the effect of moving cloud. The demand schedule analysis of the community could help the decision making of design a solar PV system in order to effectively offset the load peak for different community sectors. In this work, it is found that the solar PV array placed in C&I sector should be facing directly south, since the peak of operation for C&I is in the middle of the day, and for the residential sector, the solar should be placed facing west due to the evening peak.

References

[1] "SB-100 California Renewables Portfolio Standard Program: emissions of greenhouse gases," 10 September 2018. [Online]. Available: https://leginfo.legislature.ca.gov/faces/billNavClient.xhtml?bill_id=201720180SB100. [Accessed 08 Mar 2019].

[2] "An EPIC Approach to Deploying Advanced Energy Communities," 22 Dec 2016. [Online]. Available: https://www.lgc.org/epic-approach-advanced-energy-communities/. [Accessed 21 Feb 2017].

[3] "NREL, NREL Partners with California to Accelerate Advanced Energy Communities | Buildings |," [Online]. Available: http://www.nrel.gov/buildings/news/2016/33991. [Accessed 18 Jan 2017].

[4] K. Brecl and M. Topič, "Self-shading losses of fixed free-standing PV arrays," *Renew. Energy,* vol. 36, no. 11, p. 3211–3216, 2011.

[5] B. Celik, E. Karatepe, S. Silvestre, N. Gokmen and A. Chouder, "Analysis of spatial fixed PV arrays configurations to maximize energy harvesting in BIPV applications," *Renew. Energy,* vol. 75, p. 534–540, 2015.

[6] K. K.-L. Lau, F. Lindberg, E. Johansson, M. I. Rasmussen and S. Thorsson, "Investigating solar energy potential in tropical urban environment: A case study of Dar es Salaam, Tanzania," *Sustainable Cities and Society,* vol. 30, pp. 118-127, 2017.

[7] "NSRDB: Alphabetical List by State," [Online]. Available: http://rredc.nrel.gov/solar/old_data/nsrdb/1991-2010/hourly/list_by_state.html#C. [Accessed 18 Jan 2017].

[8] C. Deline, A. Dobos, S. Janzou, J. Meydbray and M. Donovan, "A simplified model of uniform shading in large photovoltaic arrays," *Sol. Energy,* vol. 96, p. 274–282, 2013.

[9] T. O. Kaddoura, M. A. Ramli and Y. A. Al-Turki, "On the estimation of the optimum tilt angle of PV panel in Saudi Arabia," *Renew. Sustain. Energy Rev.,* vol. 65, p. 626–634, 2016.

[10] S. Wilcox and W. Marion, "Users Manual for TMY3 Data Sets - NREL," 2008. [Online]. Available: https://www.nrel.gov/docs/fy08osti/43156.pdf.

[11] S. Harb, H. Zhang , R. S. Balog and M. Kedia, "Microinverter and string inverter grid-connected photovoltaic system — A comprehensive study," *IEEE,* pp. 2885-2890, 2013.

[12] H. Mousazadeh, A. Keyhani, A. Javadi, H. Mobli, K. Abrinia and A. Sharifi, "A review of principle and sun-tracking methods for maximizing solar systems output," *Renew. Sustain. Energy Rev.,* vol. 13, no. 8, p. 1800–1818, 2009.

[13] M. Amado and F. Poggi, "Towards Solar Urban Planning: A New Step for Better Energy Performance," *Energy Procedia,* vol. 30, pp. 1261-1273, 2012.

[14] R. Zhu, L. You, P. Santi, M. S. Wong and C. Ratti, "Solar accessibility in developing cities: A case study in Kowloon East, Hong Kong," *Sustainable Cities and Society,* 2019.

[15] M. Ouria and H. Sevinc, "Evaluation of the potential of solar energy utilization in Famagusta, Cyprus," *Sustainable Cities and Society,* vol. 37, pp. 189-202, 2018.

[16] S. Borenstein, "Private net benefits of residential solar PV: The role of electricity tariffs, tax incentives, and rebates," *Journal of the Association of Environmental and Resource Economists,* vol. 4(S1), pp. S85-S122, 2017.

[17] M. Z. Jacobson and V. Jadhav, "World estimates of PV optimal tilt angles and ratios of sunlight incident upon tilted and tracked PV panels relative to horizontal panels," *Solar Energy,* vol. 169, pp. 55-66, 2018.

[18] "HelioScope: Advanced Solar Design Software," [Online]. Available: https://www.helioscope.com/. [Accessed 09 Mar 2017].

[19] J. S. Stein, W. F. Holmgren, J. Forbess and C. W. Hansen, "PVLIB: Open source photovoltaic performance modeling functions for Matlab and Python," *IEEE,* pp. 3425-3430, 2016.

[20] J. S. Stein, "The photovoltaic Performance Modeling Collaborative (PVPMC)," in *IEEE Photovoltaic Specialists Conference,* Austin, TX, 2012.

[21] A. H. Smets, K. Jäger, O. Isabella, R. A. v. Swaaij and M. Zeman, Solar energy: the physics and engineering of photovoltaic conversion, technologies and systems, 2016.

[22] K. Jäger, O. Isabella, A. H. Smets, R. A. van Swaaij and M. Zeman, Solar Energy: Fundamentals, Technology, and Systems, UIT Cambridge, 2016.

[23] K. N. Shukla, S. Rangnekar and K. Sudhakar, "Comparative study of isotropic and anisotropic sky models to estimate solar radiation incident on tilted surface: A case study for Bhopal, India," *Energy Rep.,* vol. 1, p. 96–103, 2015.

[24] J. Rakovec and K. Zaksek, "On the proper analytical expression for the sky-view factor and the diffuse irradiation of a slope for an isotropic sky," *Renewable Energy,* vol. 37, no. 1, pp. 440-444, 2012.

[25] D. Stanciu, C. Stanciu and I. Paraschiv, "Mathematical links between optimum solar collector tilts in isotropic sky for intercepting maximum solar irradiance," *J. Atmospheric Sol.-Terr. Phys.,* vol. 137, p. 58–65, 2016.

[26] T. Muneer, C. Gueymard and H. Kambezidis, "6 - Ground Albedo," in *Solar Radiation and Daylight Models (Second Edition)*, Oxford: Butterworth-Heinemann, 2004, p. 303–316.

[27] K. Skeiker, "Optimum tilt angle and orientation for solar collectors in Syria," *Energy Convers,* vol. 50, no. 9, p. 2439–2448, 2009.

[28] Castellano, Parra, Valls-Guirado and Manzano-Agugliaro, "Optimal displacement of photovoltaic array's rows using a novel shading model," *Applied Energy,* vol. 144, pp. 1-9, 2015.

[29] S. Wilcox and W. Marion, Users manual for TMY3 data sets, Golden, CO : National Renewable Energy Laboratory, 2008.

[30] NREL, "National Solar Radiation Data Base," [Online]. Available: https://rredc.nrel.gov/solar/old_data/nsrdb/1991-2005/tmy3/by_state_and_city.html. [Accessed 21 10 2018].

[31] M. Sengupta, A. Weekley, A. Lopez and C. Molling, "Validation of the National Solar Radiation Database (NSRDB)," 2015. [Online]. Available: https://www.nrel.gov/docs/fy15osti/64981.pdf.

[32] GCL, "GCL-M6/72xxx," GCL, [Online]. Available: https://www.gclsi.com/uploads/5c1ae522/AU%20CEC-M6-72%20325-360%2035%205BB.pdf. [Accessed 12 10 2019].

[33] G. Walker, "Evaluating MPPT converter topologies using a MATLAB PV model," *Journal of Electrical & Electronics Engineering, Australia*, vol. 21, no. 1, pp. 49-55, 2001.

[34] J. Galtieri and P. T. Krein, "Designing solar arrays to account for reduced performance from self-shading," *IEEE*, pp. 1-8, 2015.

[35] A. Kajihara and A. T. Harakawa, "Model of photovoltaic cell circuits under partial shading," *IEEE*, pp. 866-870, 2005.

[36] J. A. Duffie and W. A. Beckman, Solar Engineering of Thermal Processes, Wiley, 1991.

[37] H. Patel and V. Agarwal, "MATLAB-based modeling to study the effects of partial shading on PV array characteristics," *IEEE*, vol. 23, no. 1, pp. 302-310, 2008.

[38] California Department of Forestry and Fire Protection Office of the State Fire Marshal, "Solar Photovoltaic Installation Guideline," [Online]. Available: https://osfm.fire.ca.gov/pdf/reports/solarphotovoltaicguideline.pdf. [Accessed 21 10 2019].

[39] Google Inc, "Google Project Sunroof," Google Inc, [Online]. Available: https://www.google.com/get/sunroof. [Accessed 11 03 2019].

[40] Google Inc, "Google Map," Google Inc, [Online]. Available: https://www.google.com/maps. [Accessed 05 03 2018].